

Electrocatalytic Reduction of Dioxygen to Water by Iridium Porphyrins Adsorbed on Edge Plane Graphite Electrodes

James P. Collman,* Leng Leng Chng, and David A. Tyvoll

Department of Chemistry, Stanford University, Stanford, California 94305

Received November 17, 1994[⊗]

A number of iridium porphyrins adsorbed on pyrolytic edge plane graphite electrodes have been examined for their electrocatalytic activity toward the four-electron reduction of dioxygen. Their behavior provides insight into the mechanisms by which the iridium porphyrins accomplish this electrocatalysis. Certain iridium porphyrins are found to reduce dioxygen to water via a four-electron pathway in a monometallic fashion. Axial ligation from the edge plane graphite electrode to the iridium metal center is believed to be essential for the catalytic reduction of dioxygen to occur. We propose the active species to be an Ir(II) center. The electrocatalytic behavior of all of the iridium porphyrins which have been examined can be explained by the transformation of these porphyrins to such catalytically active Ir(II) centers.

Introduction

Interest in fuel cell technology has motivated the search for an inexpensive electrode material that can accomplish the direct four-electron reduction of dioxygen to water at or near the reversible thermodynamic potential (+1.23 V vs NHE at pH 0).¹ Many macrocyclic transition metal complexes have been examined as dioxygen reduction catalysts.² Most of these reduce dioxygen (via the two-electron pathway) to hydrogen peroxide at relatively negative potentials. For an oxygen-reducing electrode to operate at or near the thermodynamic potential, hydrogen peroxide cannot be a free intermediate (the reduction potential linking hydrogen peroxide to water is +0.70 V vs NHE at pH 0).^{3a} Thus, if high efficiency is to be achieved, fuel cells must catalyze the direct reduction of dioxygen to water without the intermediate production of hydrogen peroxide. Besides the issue of efficiency, production of hydrogen peroxide—a corrosive strong oxidant—is undesirable.

To date, only a few molecular electrocatalysts have been able to achieve a direct four-electron reduction of dioxygen to water. All of these examples function only when adsorbed on edge plane graphite electrodes (EPGE). These include bis(cobalt) cofacial diporphyrins (and related systems),^{3,4} cobalt tetrakis-(4-pyridyl)porphyrin with three or four [Ru(NH₃)₅]²⁺ groups appended to the porphyrin periphery,⁵ and some iridium

octaethylporphyrin systems, e.g. Ir(OEP)H.⁶ The bis(cobalt) cofacial diporphyrins catalyze the four-electron reduction of dioxygen at relatively positive potentials ($E_{1/2}(\text{O}_2) = +0.7$ V vs NHE at pH 0).³ Dioxygen is believed to be bridging the two metal centers in the active bimetallic catalysts. The ruthenated cobalt porphyrins⁵ (which are monomeric) reduce dioxygen to water but at a much lower potential ($E_{1/2}(\text{O}_2) = +0.46$ V vs NHE at pH 0).

As a catalyst, the Ir(OEP)H investigated in our laboratories is unique.⁶ It is monomeric and yet still able to operate in acidic solutions at potentials comparable to those for the most active bis(cobalt) catalysts ($E_{1/2}(\text{O}_2) = +0.72$ V vs NHE^{6,7} at pH 1). Unlike the cofacial systems, however, the iridium catalyst becomes almost inactive at potentials less than +0.2 V vs NHE.⁷ In addition to Ir(OEP)H, several other iridium porphyrins have been examined in the past for electrocatalytic reduction of dioxygen: Ir(OEP)I, Ir(OEP)OOH, [Ir(OEP)]₂, and Ir(TTP)H.⁶ The metal–metal-bonded dimer, [Ir(OEP)]₂, was reported to have almost the same catalytic activity as monomeric Ir(OEP)H. The iodo- and hydroperoxy-iridium porphyrins were also catalytically active, but these required conditioning⁸ at reducing potentials (<−0.1 V vs NHE at pH 1⁷) to become active catalysts. Ir(TTP)H was found to show insignificant catalytic activity for dioxygen reduction.

On the basis of these studies, a mechanism was postulated for the dioxygen reduction. It was proposed that the active catalyst was actually the dimer, [Ir(OEP)]₂. This was thought to be formed upon oxidation of Ir(OEP)H at the start of the cathodic scan. To explain the loss of activity when the potential was scanned below +0.2 V vs NHE,⁷ we hypothesized that reduction of the dimer and subsequent protonation re-formed Ir(OEP)H. Thus the dimer would be stable (and therefore catalytically active) only over a limited potential range. By extension, the behavior of the other iridium catalysts could be explained: Ir(OEP)I and Ir(OEP)OOH were converted to Ir-

[⊗] Abstract published in *Advance ACS Abstracts*, February 15, 1995.

- (1) (a) Bockris, J. O'M.; Srinivasan, S. *Fuel Cells: Their Electrochemistry*; McGraw-Hill Book Co.: New York, 1969. (b) *Proceedings of the Symposium on Fuel Cells*; White, R. E., Appleby, A. J., Eds.; The Electrochemical Society Inc.: 1989.
- (2) (a) Schiffrin, D. J. *Electrochemistry* **1983**, *8*, 126–170. (b) van Veen, J. A. R.; van Baar, J. F. *Rev. Inorg. Chem.* **1982**, *4*, 293–327.
- (3) (a) Collman, J. P.; Denisevich, P.; Konai, Y.; Marrocco, M.; Koval, C.; Anson, F. C. *J. Am. Chem. Soc.* **1980**, *102*, 6027–6036. (b) Durand, R. R., Jr.; Bencosme, C. S.; Collman, J. P.; Anson, F. C. *J. Am. Chem. Soc.* **1983**, *105*, 2710–2718. (c) Collman, J. P.; Hendricks, N. H.; Kim, K.; Bencosme, C. S. *J. Chem. Soc., Chem. Commun.* **1987**, 1537–1538. (d) Chang, C. K.; Liu, H. Y.; Abdalmuhdi, I. *J. Am. Chem. Soc.* **1984**, *106*, 2725–2726. (e) Liu, H. Y.; Weaver, M. J.; Wang, C.-B.; Chang, C. K. *J. Electroanal. Chem. Interfacial Electrochem.* **1983**, *145*, 439–447. (f) Liu, H. Y.; Abdalmuhdi, I.; Chang, C. K.; Anson, F. C. *J. Phys. Chem.* **1985**, *89*, 665–670.
- (4) Collman, J. P.; Wagenknecht, P. S.; Hutchison, J. E. *Angew. Chem., Int. Ed. Engl.* **1994**, *33*, 1537–1554.
- (5) (a) Shi, C.; Anson, F. C. *J. Am. Chem. Soc.* **1991**, *113*, 9564–9570. (b) Shi, C.; Anson, F. C. *Inorg. Chem.* **1992**, *31*, 5078–5083. (c) Steiger, B.; Shi, C.; Anson, F. C. *Inorg. Chem.* **1993**, *32*, 2107–2113.

(6) (a) Collman, J. P.; Kim, K. *J. Am. Chem. Soc.* **1986**, *108*, 7847–7849. (b) Kim, K. Ph.D. Thesis, Stanford University, 1986; pp 43–79.

(7) These electrochemical data are obtained from ref 6. The electrolyte used was 0.1 M trifluoroacetic acid (TFA). The electrode was scanned at 20 mV/s, and the rotation rate was 100 rpm.

(8) The electrode can be conditioned either by holding the electrode at the conditioning potential for 3 s or by doing a linear sweep to the conditioning potential and back again to the region where dioxygen reduction occurs.

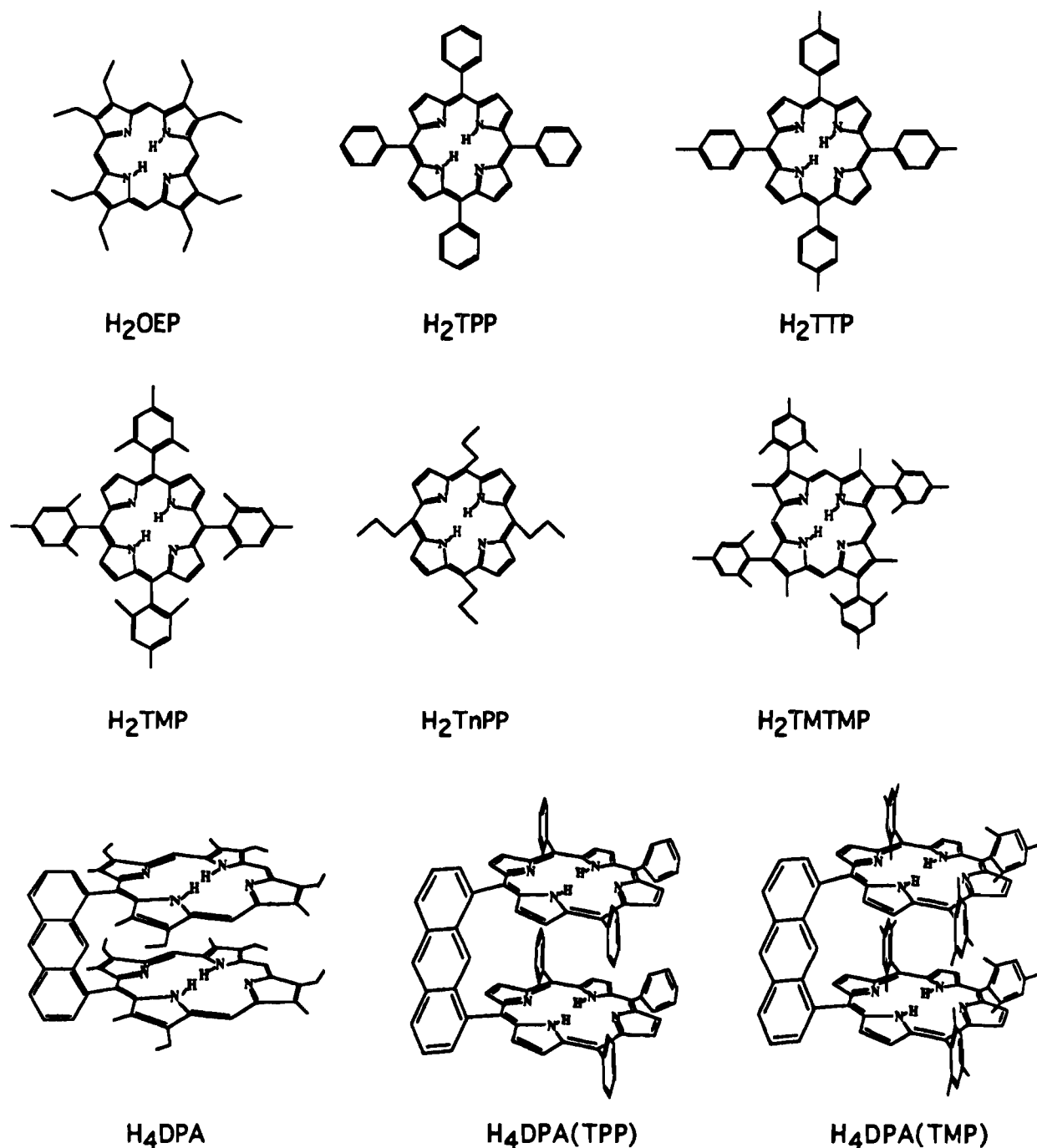


Figure 1. Structures of investigated porphyrins. H_2OEP = 2,3,7,8,12,13,17,18-octaethylporphyrin, H_2TPP = 5,10,15,20-tetraphenylporphyrin, H_2TTP = 5,10,15,20-tetratolylporphyrin, H_2TMP = 5,10,15,20-tetramesitylporphyrin, H_2TnPP = 5,10,15,20-tetra-*n*-propylporphyrin, H_2TMTMP = 2,7,12,17-tetramesityl-3,8,13,18-tetramethylporphyrin, H_4DPA = 1,8-bis(2,8,13,17-tetraethyl-3,7,12,18-tetramethylporphyrin-5-yl)anthracene, $\text{H}_4\text{DPA(TPP)}$ = 1,8-bis(10,15,20-triphenylporphyrin-5-yl)anthracene, and $\text{H}_4\text{DPA(TMP)}$ = 1,8-bis(10,15,20-trimesitylporphyrin-5-yl)anthracene.

(OEP)H at the negative conditioning potentials; Ir(TTP)H was considered too hindered to dimerize to a significant extent.

Initially, we sought to corroborate this hypothesis by examining a cofacial diporphyrin analog of Ir(TTP)H. We believed that such a species would be an efficient $4 e^-$ dioxygen reduction catalyst. Thus, $\text{Ir}_2\text{DPA(TPP)(H)}_2$ (Figure 1) was synthesized and tested for its reactivity. Its unexpected behavior led us to expand our studies considerably.

In the present report, several families of iridium porphyrins have been prepared and examined for their catalytic activities toward dioxygen reduction on EPGE. In so doing, we hoped to address the following questions: (1) Is the axial ligand stable throughout the catalysis? (2) What is the nature of the graphite-catalyst interaction? (3) How does the catalyst respond when

the redox properties of the porphyrin are varied? (4) How does the catalyst respond when the steric properties of the porphyrin are varied? In other words, is the catalysis actually bimetallic? Some of the catalysts that were examined earlier were reinvestigated. The present results provide insight into the mechanisms by which these iridium porphyrins adsorbed on EPGE catalyze the four-electron reduction of dioxygen.

Results

The structures of the porphyrins used in this study are shown in Figure 1. All potentials reported are vs SCE at pH 1.

Synthesis. The $[\text{Ir}(\text{OEP})_2]$ that has been examined in the present study was obtained from photolysis of $\text{Ir}(\text{OEP})\text{CH}_2\text{Ph}$

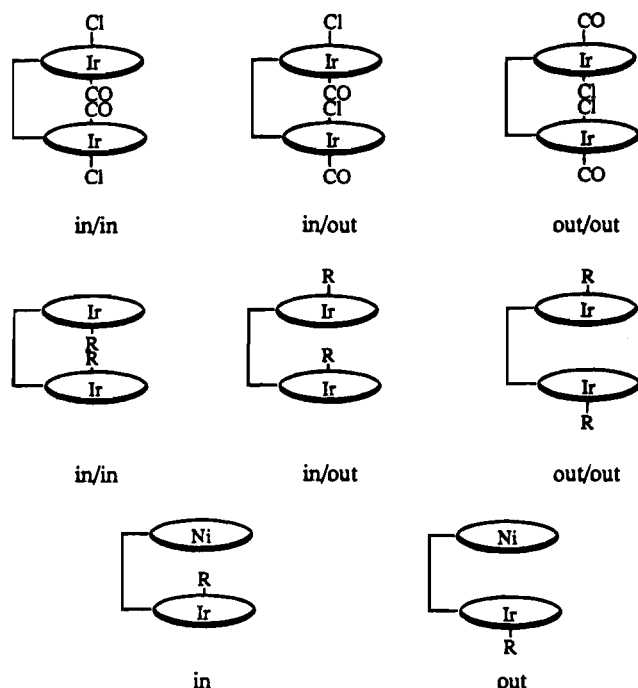


Figure 2. Regioisomers of the cofacial mono- and diiridium porphyrins.

in C_6D_6 . By 1H NMR, the resulting dimer appears to be free from both $Ir(OEP)H$ and $Ir(OEP)CH_2Ph$.

The hydrides of these iridium porphyrins are air-sensitive (particularly when in solution). $Ir(OEP)H$ is known to react slowly with dioxygen in solution to form $Ir(OEP)OOH$.⁶ Thus, these porphyrins have been handled and stored in an inert-atmosphere box. The iridium alkyl and aryl porphyrins are relatively stable in the presence of air, and they need not be purified in an inert-atmosphere box. However, when they are in solution, exposed to light, air, or water, these complexes slowly decompose over time. Thus, these porphyrins were also stored in the drybox.

The cofacial diporphyrin complexes $Ir_2DPA(H)_2$, $Ir_2DPA(TPP)(H)_2$, and $Ir_2DPA(TMP)(H)_2$ were synthesized in a manner similar to that used for the monomers (i.e. $Ir(OEP)H$,⁹ $Ir(TPP)H$, and $Ir(TMP)H$). A mixture of three isomers was produced in each cofacial diporphyrin—the in/in, in/out, and out/out regioisomers (Figure 2). No attempts were made to separate these isomers, and they have been examined as a mixture to measure their activities toward dioxygen reduction.

The iridium alkyl dimeric porphyrins, $Ir_2DPA(C_2H_5)_2$ and $Ir_2DPA(CH_3)_2$, were also produced as a mixture of three isomers—the in/in, the in/out, and the out/out isomers. The in/out and the out/out isomers were separated by preparative TLC and each isomer was examined separately for its catalytic activity. The in/in isomer has yet to be isolated.

Heterometallic cofacial diporphyrins have been synthesized as shown in Scheme 1. $Ir(Ni)DPA(CH_3)$ and $Ir(Ni)DPA(C_2H_5)$ gave the expected mixture of two isomers (Figure 2); these were separated on preparative TLC and examined individually on the rotating disk electrode.

Catalyzed Dioxygen Reduction by $Ir(OEP)$ Porphyrins. Table 1 summarizes the reactivities of the $Ir(OEP)$ porphyrin derivatives toward dioxygen reduction. With the exception of $Ir(OEP)C_6H_3(CF_3)_2$, all the other $Ir(OEP)R$ porphyrins (where $R = H$, alkyl, or aryl) catalyze the four-electron reduction of dioxygen to water. $Ir(OEP)H$ does not require any conditioning;

it starts to reduce dioxygen at +0.56 V (Figure 3). The other $Ir(OEP)$ alkyl or aryl porphyrins will only reduce dioxygen after they have been conditioned⁸ at a positive potential ($>+0.8$ V) (Figure 4). Conditioning at negative potentials does not yield any significant reduction current in the region where dioxygen reduction usually occurs. The conditioning potential required to produce significant dioxygen reduction current varies depending upon the nature of the alkyl or aryl group bound to the iridium metal. The limiting current obtained for the dioxygen reduction after the catalysts have been conditioned also depends upon the porphyrins being examined. The required conditioning potentials vary as follows: $i-Pr$, $-CH_2Ph$, $Et < Me < -C_6H_3(CH_3)_2 < Ph < -C_6H_3(CF_3)_2$. In contrast, the limiting currents of the resulting electrocatalysts follow the opposite trend: $i-Pr$, $-CH_2Ph$, $Et > Me > -C_6H_3(CH_3)_2 > Ph > -C_6H_3(CF_3)_2$. $Ir(OEP)C_6H_3(CF_3)_2$ does not become an active catalyst regardless of the applied conditioning potential (positive or negative).

The $[Ir(OEP)]_2$ examined in this study is also a four-electron catalyst for dioxygen reduction. However, it starts to reduce dioxygen at a lower potential compared to $Ir(OEP)H$ (Figure 5). Upon negative conditioning at -1 V, the dimer becomes a much better catalyst in terms of its limiting current. It also starts to reduce dioxygen at a more positive potential after negative conditioning (Figure 5).

Catalyzed Dioxygen Reduction by Monomeric Iridium Hydride Porphyrins. The catalytic activities of the Ir -(monomer) H porphyrins (monomer = OEP, TPP, TTP, TnPP, TMP, TMTMP) toward dioxygen reduction are summarized in Table 2. $Ir(TMP)H$ and $Ir(TMTMP)H$ are inactive toward dioxygen reduction. $Ir(TPP)H$, $Ir(TTP)H$, and $Ir(TnPP)H$ do catalyze the reduction of dioxygen to water when these catalysts are scanned from +0.8 to 0 V. However, their activities die rapidly (Figure 6). Upon negative conditioning (at -1 V), their catalytic capabilities increase dramatically (Figure 7). On the other hand, the catalytic activity of $Ir(OEP)H$ diminishes only slowly when it is scanned from +0.8 to 0 V. (Negative conditioning does not increase its catalytic activity in this case.)

Catalyzed Dioxygen Reduction by Cofacial Diiridium Diporphyrins Dihydrides. As shown in Table 3, $Ir_2DPA(H)_2$ and $Ir_2DPA(TPP)(H)_2$ reduce dioxygen to water, whereas $Ir_2DPA(TMP)(H)_2$ is inactive. Compared to those of their monomeric analogs ($Ir(OEP)H$ and $Ir(TPP)H$), the limiting currents and the $E_{1/2}(O_2)$ values of $Ir_2DPA(H)_2$ and $Ir_2DPA(TPP)(H)_2$ are lower.

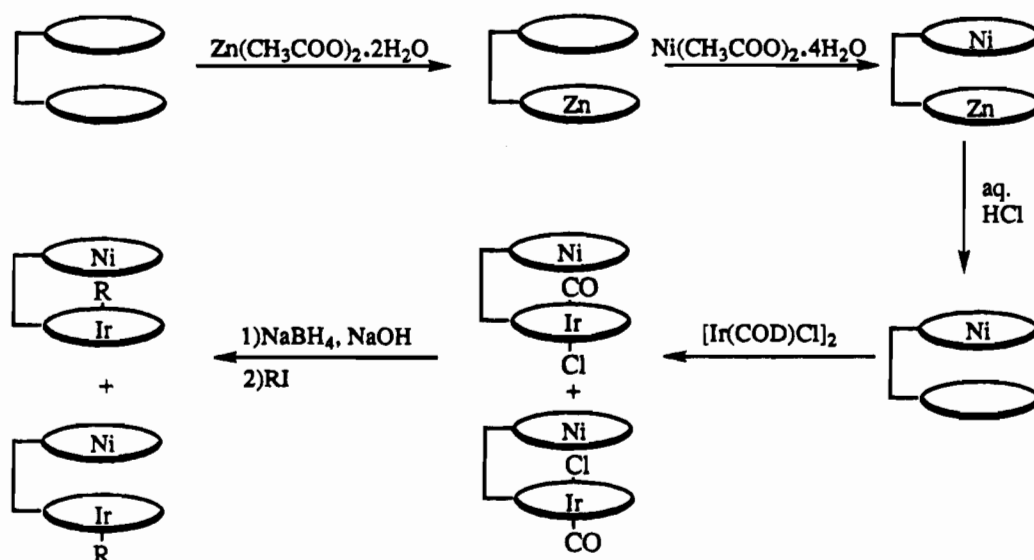
Catalyzed Dioxygen Reduction by Cofacial Bis(alkyliridium) Diporphyrins and Cofacial Mononickel Mono(alkyliridium) Diporphyrins. As shown in Table 4, $Ni(Ir)DPA(CH_3)$ -in and $Ni(Ir)DPA(C_2H_5)$ -in become active catalysts for the four-electron reduction of dioxygen after positive conditioning whereas $Ni(Ir)DPA(CH_3)$ -out and $Ni(Ir)DPA(C_2H_5)$ -out are not active, even after positive conditioning. Unlike $Ir(OEP)CH_3$ and $Ir(OEP)C_2H_5$, $Ni(Ir)DPA(CH_3)$ -in and $Ni(Ir)DPA(C_2H_5)$ -in do become active catalysts after undergoing negative conditioning (at -2 V).

The $Ir_2DPA(CH_3)_2$ -in/out isomer and the $Ir_2DPA(C_2H_5)_2$ -in/out isomer can catalyze the reduction of dioxygen to water after positive conditioning whereas both out/out isomers are inactive.

Dependence of Catalytic Activity of $Ir(OEP)H$ on Surface Coverage. When the amount of $Ir(OEP)H$ that is applied to the EPGE is decreased to ca. 6.5×10^{-10} mol cm^{-2} of geometric electrode area, two reduction waves can be seen (Figure 8)—one wave at a higher overpotential and the other at a lower overpotential. The reduction current at the lower overpotential disappears completely if the amount of catalyst that is applied

(9) Ogoshi, H.; Setsune, J.-I.; Yoshida, Z.-I. *J. Organomet. Chem.* **1978**, *159*, 317–328.

Scheme 1

**Table 1.** Dioxygen Reduction Catalyzed by Ir(OEP) Porphyrins

compound	$E_{1/2}(\text{O}_2)^a$	I_{lim}^b	4 e ⁻ catalyst? ^c	conditioning? ^d
Ir(OEP)H	0.38	2.0	yes	no
Ir(OEP)- <i>i</i> -Pr	0.35	2.3	yes	yes (0.8–1.2)
Ir(OEP)CH ₂ Ph	0.32	2.3	yes	yes (0.8–1.3)
Ir(OEP)Et	0.34	2.0	yes	yes (0.8–1.3)
Ir(OEP)Me	0.31	1.6	yes	yes (1–1.3)
Ir(OEP)C ₆ H ₃ (CH ₃) ₂ ^e	0.30	0.5	yes	yes (1–1.4)
Ir(OEP)Ph	0.30	0.2	yes	yes (1–1.4)
Ir(OEP)C ₆ H ₃ (CF ₃) ₂ ^f			no	
[Ir(OEP)] ₂	0.31, ^g 0.33 ^h	1.3, ^g 1.9 ^h	yes	yes (–1)
Ir(OEP)I	0.29	1.3	yes	yes (–0.2)
Ir(OEP)OOH	0.30	1.1	yes	yes (–0.2)

^a $E_{1/2}(\text{O}_2)$ is the half-wave potential for the dioxygen reduction found from rotating disk electrode (RDE) experiments (all potentials in V vs SCE) at a rotation rate of 1600 and a scan rate of 100 mV/s. Electrolyte used is 0.1 M trifluoroacetic acid (TFA), saturated with dioxygen. ^b I_{lim} is the limiting current in mA from RDE experiments at a rotation rate of 1600 and a scan rate of 100 mV/s. ^c Determined by rotating ring-disk electrode (RRDE) experiments. ^d All potentials in V vs SCE. ^e C₆H₃(CH₃)₂ is 3,5-dimethylphenyl. ^f C₆H₃(CF₃)₂ is 3,5-bis(trifluoromethyl)phenyl. ^g Before negative conditioning. ^h After negative conditioning.

is reduced to ca. 10⁻¹⁰ mol cm⁻², while the one at higher overpotential still remains at lower coverages.

Discussion

Synthesis. The metal–metal-bonded dimer [Ir(OEP)]₂, previously synthesized in our laboratories and examined for its catalytic activity toward dioxygen reduction contained ca. 10% of Ir(OEP)H.⁶ Originally it was prepared by photolysis of Ir(OEP)H in toluene. Subsequently in 1986 Wayland et al. reported that [Ir(OEP)]₂ reacts with neat toluene when heated to form Ir(OEP)H and Ir(OEP)CH₂Ph.¹⁰ Thus when the photolysis of the Ir(OEP)H was carried out in toluene, the resulting dimer could react with the solvent to produce more starting material Ir(OEP)H (e.g. when the photolysis cell was not cooled properly). Since these iridium porphyrins are extraordinarily active electrode catalysts, small amounts of impurities can mask other catalytic effects entirely.

We wished to examine the catalytic behavior of the pure dimer without Ir(OEP)H contamination. Wayland et al. have successively synthesized [Ir(OEP)]₂ from Ir(OEP)CH₃ by photolysis in C₆D₆.^{10,11} In this study, we have obtained the dimer by photolyzing Ir(OEP)CH₂Ph in C₆D₆. (Ir(OEP)CH₂Ph itself

is a four-electron catalyst of dioxygen reduction but only after conditioning at positive potential; vide supra.) No Ir(OEP)H could be detected by ¹H NMR.

Iridium insertion⁹ into the cofacial diporphyrins H₄DPA, H₄DPA(TPP), and H₄DPA(TMP) produces Ir₂DPA(CO)₂(Cl)₂, Ir₂DPA(TPP)(CO)₂(Cl)₂, and Ir₂DPA(TMP)(CO)₂(Cl)₂, respectively. Three regioisomers are obtained for each case—the in/in, the in/out, and the out/out (Figure 2). For each of the above compounds, two bands can be isolated using chromatography. These bands can subsequently be reduced to the dihydrides or alkylated to form the dialkyls. Regardless of which band was used, a mixture of the same three regioisomers was again obtained. For the dihydride species, the three isomers were not separated, and in the upfield region (from –57 to –61 ppm), a number of hydride signals can be seen for Ir₂DPA(H)₂, Ir₂DPA(TPP)(H)₂, and Ir₂DPA(TMP)(H)₂.

For Ir₂DPA(CH₃)₂ and Ir₂DPA(C₂H₅)₂, the out/out (major) and the in/out (minor) isomers can be isolated for each case and identified on the basis of their ¹H NMR spectra. For example, the Ir₂DPA(CH₃)₂-out/out isomer has symmetric C_{2v} symmetry and the axial methyl groups experience a diamagnetic anisotropic shift that results predominantly from only one porphyrin ring. This can be seen from its ¹H NMR spectrum, which exhibits a C_{2v} symmetry and has a single upfield signal at –6.81 ppm. For comparison, the axial methyl signal for Ir(OEP)CH₃ appears at –6.38 ppm. The Ir₂DPA(CH₃)₂-in/out isomer has unsymmetric C_s symmetry. One methyl group resides outside the diporphyrin cavity and likewise experiences a diamagnetic anisotropic shift that results predominantly from only one porphyrin ring. The other methyl group is found inside the cavity and thus experiences a strong anisotropic shift from both porphyrin rings. The ¹H NMR spectrum of this compound does indeed exhibit C_s symmetry, and it has two methyl signals in the upfield region, at –6.82 and –12.98 ppm. The peak at –6.82 ppm is assigned to the methyl group ligated to the iridium metal outside of the cavity while the peak at –12.98 ppm is assigned to the methyl group inside the diporphyrin cavity. Similar reasoning has been used to assign the two bands that are isolated for Ir₂DPA(C₂H₅)₂. The in/in isomers for both Ir₂

(10) Del Rossi, K. J.; Wayland, B. B. *J. Chem. Soc., Chem. Commun.* **1986**, 1653–1655.

(11) Recently, [Ir(OEP)]₂ was also prepared by the reaction of 2,2,6,6-tetramethyl-1-piperidinyloxy (TEMPO) with Ir(OEP)H: Chan, K. S.; Leung, Y.-B. *Inorg. Chem.* **1994**, *33*, 3187.

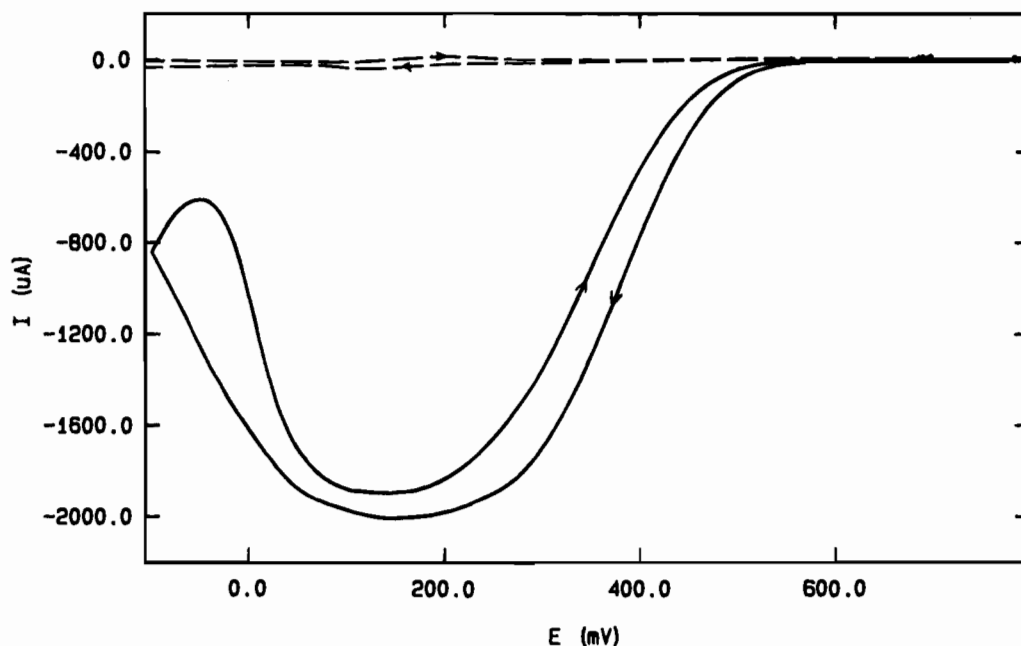


Figure 3. Rotating-disk cyclic voltammograms for a pyrolytic EPGE coated with Ir(OEP)H in the presence (solid line) and absence (dashed line) of O_2 : supporting electrolyte 0.1 M TFA; scan rate 100 mV/s; rotation rate 1600 rpm.

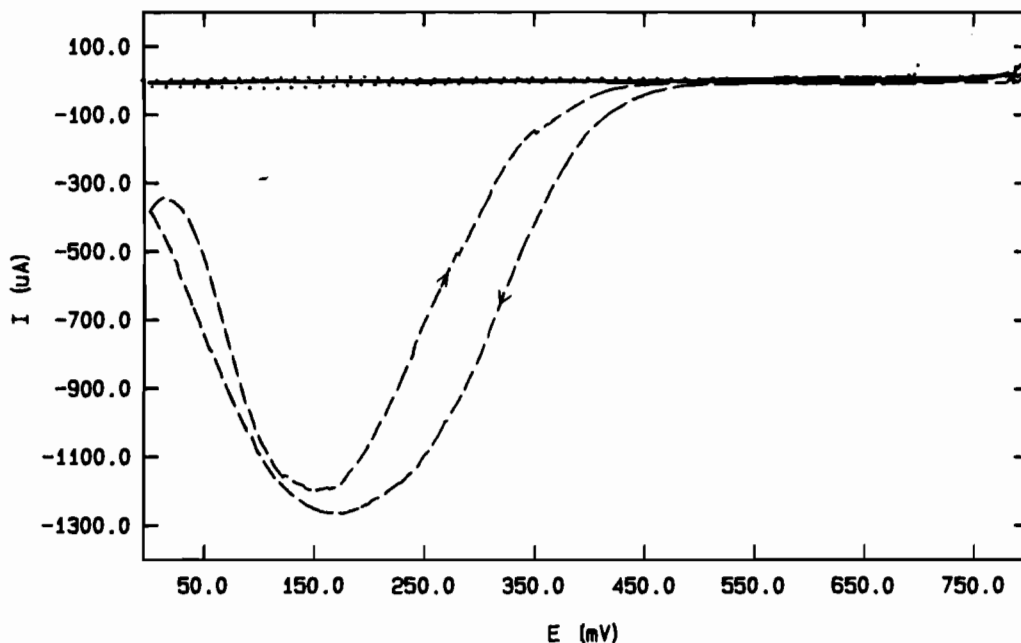


Figure 4. Rotating-disk cyclic voltammograms for a pyrolytic EPGE coated with Ir(OEP)CH₂Ph: supporting electrolyte 0.1 M TFA; scan rate 100 mV/s; rotation rate 1600 rpm. The solid line shows the result before conditioning in the presence of O_2 , and the dashed line shows the result after conditioning (conditioning potential 1.2 V vs SCE; conditioning time 3 s) in the presence of O_2 . The dotted shows the result after conditioning in the absence of O_2 .

DPA(CH₃)₂ and Ir₂DPA(C₂H₅)₂ have not been isolated—they were probably formed in very small quantities.

The mixed-metal cofacial diporphyrins Ni(Ir)DPA(CH₃) and Ni(Ir)DPA(C₂H₅) were synthesized as a mixture of two regioisomers, respectively—the in (minor product) and the out (major product) isomers (Figure 2). These isomers were separated and identified on the basis of their ¹H NMR spectra. For Ni(Ir)-DPA(CH₃)-out, the methyl signal appears at -6.76 ppm; the methyl signal of Ni(Ir)DPA(CH₃)-in appears at -10.01 ppm. The Ni(Ir)DPA(C₂H₅)-in and -out isomers were similarly identified.

Catalyzed Dioxygen Reduction by Ir(OEP) Porphyrins.

In our earlier report, [Ir(OEP)]₂ was believed to be the active catalyst on the surface of the graphite (the dimer was contami-

nated with 10% Ir(OEP)H). In the present work, [Ir(OEP)]₂ was synthesized via another precursor, Ir(OEP)CH₂Ph. This dimer behaves fundamentally differently from its predecessor. While it does reduce dioxygen to water, the catalysis occurs at a greater overpotential. Specifically, the dioxygen reduction with [Ir(OEP)]₂ begins at +0.40 V compared to +0.56 V for Ir(OEP)H. When the dimer is conditioned at a negative potential (-1 V), it starts to reduce dioxygen at a more positive potential (+0.48 V) and the limiting current also increases (Figure 5). This implies that the [Ir(OEP)]₂ itself cannot be the active catalyst; rather, it is a precatalyst. The catalytic activity reported for the dimer in our earlier report was very probably due to the 10% impurity (i.e. Ir(OEP)H) that was present in the dimer.¹²

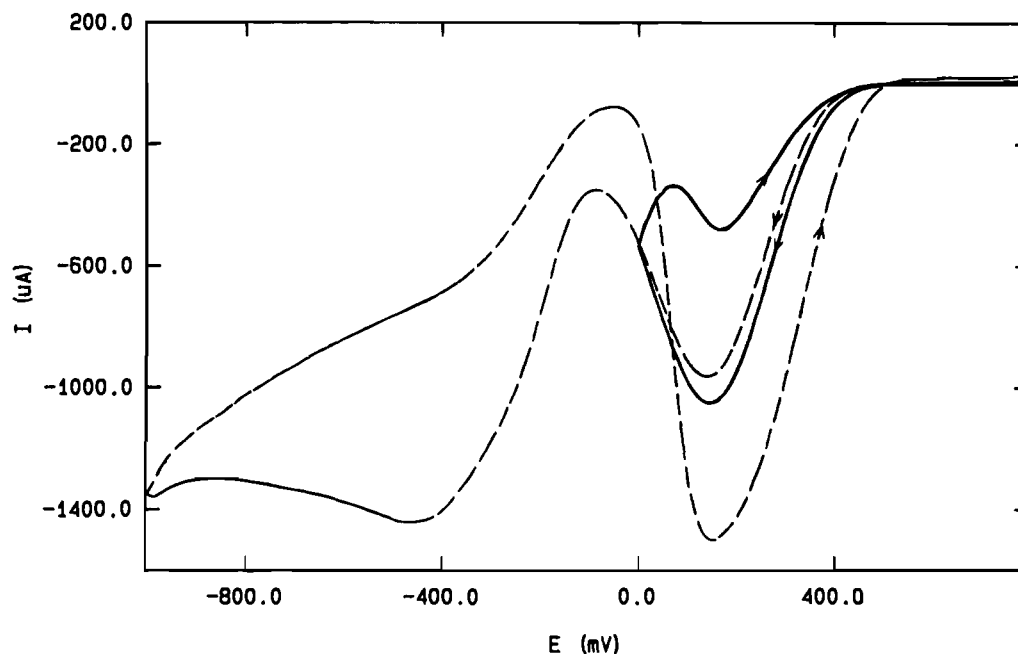


Figure 5. Rotating-disk cyclic voltammograms for the reduction of O_2 at a pyrolytic EPGE on which $[Ir(OEP)]_2$ is adsorbed: supporting electrolyte 0.1 M TFA saturated with O_2 ; scan rate 100 mV/s; rotation rate 1600 rpm. The solid line shows the result before negative conditioning, and the dashed line shows the result after negative conditioning at -1 V vs SCE.

Table 2. Dioxygen Reduction Catalyzed by Ir(monomer)H Porphyrins

compound	$E_{1/2}(O_2)^a$	I_{lim}^b	$4 e^-$ catalyst? ^c	conditioning? ^d
Ir(OEP)H	0.38	2.0	yes	no
Ir(TPP)H	0.24	1.8	yes	yes (-)
Ir(TTP)H	0.21	2.0	yes	yes (-)
Ir(TMP)H			no	
Ir(TMTMP)H			no	
Ir(TnPP)H	0.28	2.3	yes	yes (-)

^a $E_{1/2}(O_2)$ is the half-wave potential for the dioxygen reduction found from RDE experiments (all potentials in V vs SCE) at a rotation rate of 1600 and a scan rate of 100 mV/s. Electrolyte used is 0.1 M trifluoroacetic acid (TFA), saturated with dioxygen. ^b I_{lim} is the limiting current in mA from RDE experiments at a rotation rate of 1600 and a scan rate of 100 mV/s. ^c Determined by RRDE experiments. ^d All potentials in V vs SCE.

For the family of monomeric Ir(OEP)R porphyrins (where R = H, alkyl, or aryl), all are four-electron catalysts for dioxygen reduction except Ir(OEP) $C_6H_3(CF_3)_2$ (Table 1). Unlike Ir(OEP)H, however, which does not require conditioning, the rest of the Ir(OEP)R porphyrins (R = alkyl or aryl) are precatalysts; they become active only after conditioning at positive potentials. Organometallic compounds of this type are known to undergo metal-carbon bond cleavage upon electrochemical oxidation by one electron.¹³ This produces a positively charged metal center and a carbon radical. The relative stabilities of carbon radicals are well-known:¹⁴ $3^\circ > 2^\circ > 1^\circ > \text{aryl}$ (electron-donating groups on the aryl radical stabilize the species while electron-withdrawing groups destabilize it.) Both the trends of the conditioning potentials required to activate the various alkylated Ir(OEP) porphyrins and the limiting catalytic currents

correlate with the stability of the expected carbon radicals. This suggests that in order for the Ir(OEP)R porphyrins to become active four-electron catalysts for dioxygen reduction, the iridium-carbon bond must be cleaved. This could occur at a positive conditioning potential ($> +0.8$ V) to generate a positively charged Ir(III) center and a carbon radical. Upon scanning to a more negative potential where the dioxygen reduction occurs (ca. $+0.4$ V), the Ir(III) center would be reduced to Ir(II) which could then interact with dioxygen (either in a monometallic or a bimetallic fashion) and reduce it catalytically.

Ir(OEP)H does not require conditioning at a positive potential to become an active catalyst. Apparently this is because it can be oxidized much more easily to yield an Ir(II) center and a proton. (The formal redox potential of Ir(OEP)H in the absence of dioxygen was reported to be ca. $+0.14$ V.^{6,7} This occurs at a potential ca. 460 mV more negative than the start of the cathodic disk current.) Thus, Ir(OEP)H is also technically a precatalyst, but its required conditioning potential is much lower—well within the bounds of the experimental potential scan. Ir(OEP) $C_6H_3(CF_3)_2$ never becomes an active catalyst even after conditioning. Presumably the strong iridium-carbon bond and the instability of the $C_6H_3(CF_3)_2$ radical prevent the generation of the active Ir(II) center.

Two features of the Ir(OEP)R (R = alkyl or aryl) porphyrins are worth addressing at this point. After these precatalysts underwent the required conditioning at positive potentials, their $E_{1/2}(O_2)$ values were found to be slightly less positive than that of Ir(OEP)H (Table 1). This difference might be attributed to degradation of the adsorbed catalysts at such strongly oxidizing potentials ($> +1.2$ V). It is also important to recognize that the values listed for the various conditioning potentials are representative ranges only. The catalysis is not an "on/off" phenomenon; for any given conditioning potential a change of even 100 mV will affect the ensuing catalytic wave. In general, the wave will be enhanced or diminished, but seldom will it become present/absent entirely. Thus there is an inherent arbitrariness in the reported values. We have tried to be consistent in their determinations; in general we report the range which leads to the highest subsequent limiting current.

(12) In ref 6, we originally reported that both Ir(OEP)H and $[Ir(OEP)]_2$ on graphite exhibit the same redox wave under N_2 . In the present study, $[Ir(OEP)]_2$ does not exhibit the same surface voltammogram as Ir(OEP)H in the absence of O_2 .

(13) Pickett, C. J. *The Chemistry of the Metal-carbon Bond*; Hartley, F. R., Patai, S., Eds.; John Wiley & Sons: New York, 1985; Vol. 2, Chapter 1, pp 1-24.

(14) McMurry, J. *Organic Chemistry*, 3rd ed.; Brooks/Cole Publishing Co.: 1992; pp 230-232.

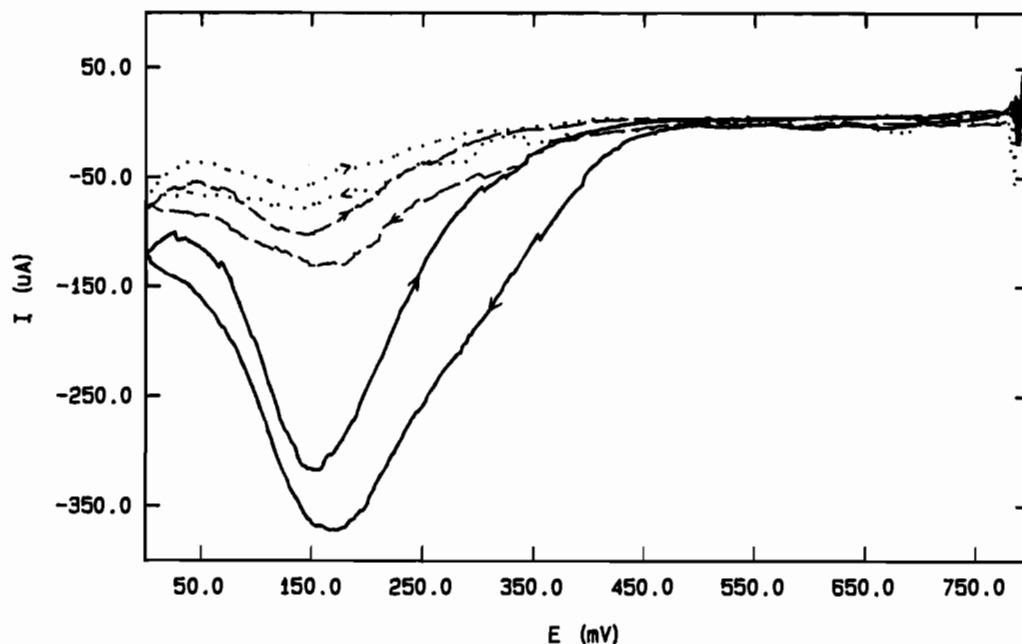


Figure 6. Rotating-disk cyclic voltammograms for the reduction of O_2 at a pyrolytic EPGE on which Ir(TPP)H is adsorbed: supporting electrolyte 0.1 M TFA saturated with O_2 ; scan rate 100 mV/s; rotation rate 1600 rpm. The solid line shows the first scan, the dashed line the second scan, and the dotted line the third scan.

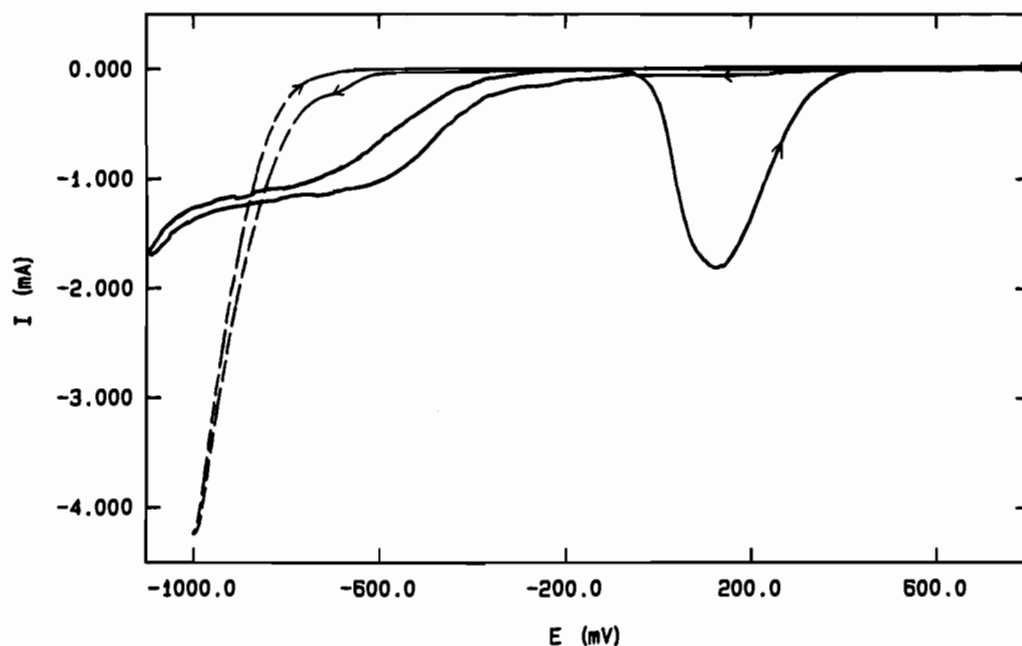


Figure 7. Rotating-disk cyclic voltammograms for a pyrolytic EPGE coated with Ir(TPP)H in the presence (solid line) and absence (dashed line) of O_2 : supporting electrolyte 0.1 M TFA; scan rate 100 mV/s; rotation rate 1600 rpm. The catalyst has been conditioned at -1 V vs SCE.

Ir(OEP)I and Ir(OEP)OOH become active catalysts after *negative* conditioning. We propose that reduction at these negative potentials causes a rupture of the Ir–I or the Ir–OOH bond, generating the active Ir(II) center and an iodide or a hydroperoxide anion. The Ir(II) center thus formed can then reduce dioxygen.

For all the active iridium catalysts mentioned above, virtually no hydrogen peroxide is detected by rotating ring-disk analysis until the disk potential reaches 0 V. In our earlier studies,⁶ Ir(OEP)H was found not to reduce H_2O_2 in the absence of dioxygen. Thus, all the active catalysts mediate a direct four-electron reduction of dioxygen to water. This stands in contrast to the cofacial cobalt systems, which slowly reduce H_2O_2 .^{3d,f,15}

Dependence of Catalytic Activity of Ir(OEP)H on Surface Coverage. When the amount of Ir(OEP)H on the EPGE

decreases to ca. 5×10^{-10} mol cm^{-2} of geometric electrode area, two reduction waves can be seen—one at a higher overpotential and the other at a lower overpotential (Figure 8). Upon repeated scanning at negative potentials, the lower overpotential wave disappears entirely. We envision at least two possibilities that could explain this phenomenon:

(1) The EPGE contains oxygenated functional groups on the surface, e.g. quinones, phenols, carboxylic acids, lactones, and carbonyls.¹⁶ These groups may act as axial ligands to coordinate to the iridium when the metalloporphyrin is adsorbed onto the EPGE. The monomer, Ir(OEP)H, may have different affinities for different functional groups due to their varying ligating


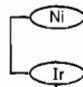
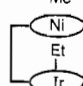
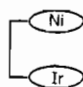
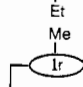
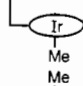
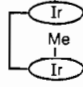
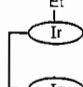
(15) Collman, J. P.; Hendricks, N. H.; Leidner, C. R.; Ngameni, E.; L'Her, M. *Inorg. Chem.* **1988**, *27*, 387–393.

Table 3. Dioxygen Reduction Catalyzed by Cofacial Diiridium Diporphyrin Dihydrides

compound	$E_{1/2}(\text{O}_2)^a$	I_{lim}^b	4 e ⁻ catalyst? ^c	conditioning? ^d
Ir ₂ DPA(H) ₂	0.29	0.69	yes	no
Ir ₂ DPA(TPP)(H) ₂	0.19	0.20	yes	yes (-1)
Ir ₂ DPA(TMP)(H) ₂			no	

^a $E_{1/2}(\text{O}_2)$ is the half-wave potential for the dioxygen reduction found from RDE experiments (all potentials in V vs SCE) at a rotation rate of 1600 and a scan rate of 100 mV/s. Electrolyte used is 0.1 M trifluoroacetic acid (TFA), saturated with dioxygen. ^b I_{lim} is the limiting current in mA from RDE experiments at a rotation rate of 1600 and a scan rate of 100 mV/s. ^c Determined by RRDE experiments. ^d All potentials in V vs SCE.

Table 4. Dioxygen Reduction Catalyzed by Cofacial Bis(alkyliridium) Diporphyrins and Cofacial Mononickel Mono(alkyliridium) Diporphyrins

compound	$E_{1/2}(\text{O}_2)^a$	I_{lim}^b	4 e ⁻ catalyst? ^c	conditioning? ^d
	0.32 ^e 0.29 ^f	0.10 ^e 0.24 ^f	yes	yes (1-1.2) yes (-0.5 to -3)
			no	
	0.32 ^e 0.37 ^f	0.50 ^e 1.2 ^f	yes	yes (0.9-1.1) yes (-0.6 to -2)
			no	
			no	
	0.31	0.25	yes	yes (0.9-1.1)
			no	
	0.30	0.47	yes	yes (0.9-1.1)

^a $E_{1/2}(\text{O}_2)$ is the half-wave potential for the dioxygen reduction found from RDE experiments (all potentials in V vs SCE) at a rotation rate of 1600 and a scan rate of 100 mV/s. Electrolyte used is 0.1 M trifluoroacetic acid (TFA), saturated with dioxygen. ^b I_{lim} is the limiting current in mA from RDE experiments at a rotation rate of 1600 and a scan rate of 100 mV/s. ^c Determined by RRDE experiments. ^d All potentials in V vs SCE. ^e After positive conditioning. ^f After negative conditioning.

abilities as well as their relative accessibility on the electrode surface. When coordinated to the iridium metal, these different axial ligands could affect the dioxygen reduction potential. In any event, distinct chemical sites may exist on the electrode. At submonolayer coverage, the adsorption process of Ir(OEP)H may lead to preferential occupation of a particular site. The catalytic reduction wave at a higher overpotential could arise

when Ir(OEP)H is ligated to those functional groups which are more accessible or have stronger coordinating affinities. When the surface coverage is increased, the Ir(OEP)H would then adsorb onto the other sites (which are less accessible or have lower affinities, but improve the catalyst overpotential), thus enabling the resulting catalyst to reduce dioxygen at a lower overpotential. At very high surface coverage, the two waves superimpose to produce a single reduction wave.

(2) Alternatively, the monomer, Ir(OEP)H, could catalyze the reduction of dioxygen via two different mechanisms—one involving a bimetallic pathway and the other requiring only a single metal center. At high surface coverage, the metal centers could approach each other and the concerted action of two iridium metals on dioxygen would lead to a catalytic wave at a lower overpotential. At low surface coverage, the mechanism of dioxygen reduction would be dominated by a monometallic pathway giving rise to the reduction wave at a higher overpotential.

Catalyzed Dioxygen Reduction by Monomeric Iridium Hydride Porphyrins. The Ir(monomer)H porphyrins vary in their abilities to catalyze dioxygen reduction. When Ir(TPP)H, Ir(TTP)H, and Ir(TnPP)H are scanned between +0.8 and 0 V, they do catalyze the reduction of dioxygen to water (with small limiting currents), but their catalytic activities diminish very rapidly (Figure 6). Upon conditioning at negative potentials, however, dioxygen reduction catalysis increases dramatically (Table 2, Figure 7). Positive conditioning does not restore or improve the catalysis. The mesityl-substituted porphyrins, Ir-(TMP)H and Ir(TMTMP)H, are entirely inactive toward dioxygen reduction on EPGE; neither positive nor negative conditioning leads to any improvement.

The aryl-substituted metalloporphyrins vary in the steric demands of the different porphyrin ligands. Ir(TMP)H and Ir-(TMTMP)H are the most sterically hindered and are believed not to be able to form metal-metal bonds.¹⁷ By extension, even the close proximity of two such iridium porphyrins is disfavored. An interaction between the iridium atom and any functional group present on the graphite surface would be similarly disfavored.

The Ir(monomer)H porphyrins vary in their electronic properties as well; in turn, many of these properties are conferred on the metal center. The porphyrins being investigated vary as shown, with OEP being the most electron-donating and TPP being the most electron-withdrawing: OEP > TMTMP > TnPP > TMP > TTP > TPP.¹⁸ Thus, it is easiest to oxidize Ir(OEP)H. This trend is consistent with the hypotheses in the preceding paragraphs. Ir(TPP)H, Ir(TTP)H, and Ir(TnPP)H undergo reduction much more easily; at negative potentials, they should be reduced to [Ir(monomer)H]⁻. This species could then be protonated in the acidic medium to yield dihydrogen and the active Ir(II) center (in a related system, we have shown that [Ru(OEP)(THF)H]⁻ can be protonated in solution by an organic acid to form Ru(OEP)(THF)(H₂), which will release dihydrogen¹⁹).

Catalyzed Dioxygen Reduction by Cofacial Diiridium Diporphyrins Dihydrides.

The investigations of Ir₂DPA(H)₂,

- (16) (a) Leon y Leon D., C. A.; Radovic, L. R. *Chemistry and Physics of Carbon*, Vol. 24; Thrower, P. A., Ed.; Marcel Dekker, Inc.: New York, 1994; Chapter 4, pp 213-310. (b) Kinoshita, K. *Carbon Electrochemical and Physicochemical Properties*; John Wiley & Sons: New York, 1988; Chapter 3, pp 86-139.
- (17) (a) Camenzind, M. J.; James, B. R.; Dolphin, D. J. *Chem. Soc., Chem. Commun.* **1986**, 1137-1139. (b) Sherry, A. E.; Wayland, B. B. *J. Am. Chem. Soc.* **1989**, *111*, 5010-5012.
- (18) Worthington, P.; Hambright, P.; Williams, R. F. X.; Reid, J.; Burnham, C.; Shamim, A.; Turay, J.; Bell, D. M.; Kirkland, R. *J. Inorg. Biochem.* **1980**, *12*, 281-291.

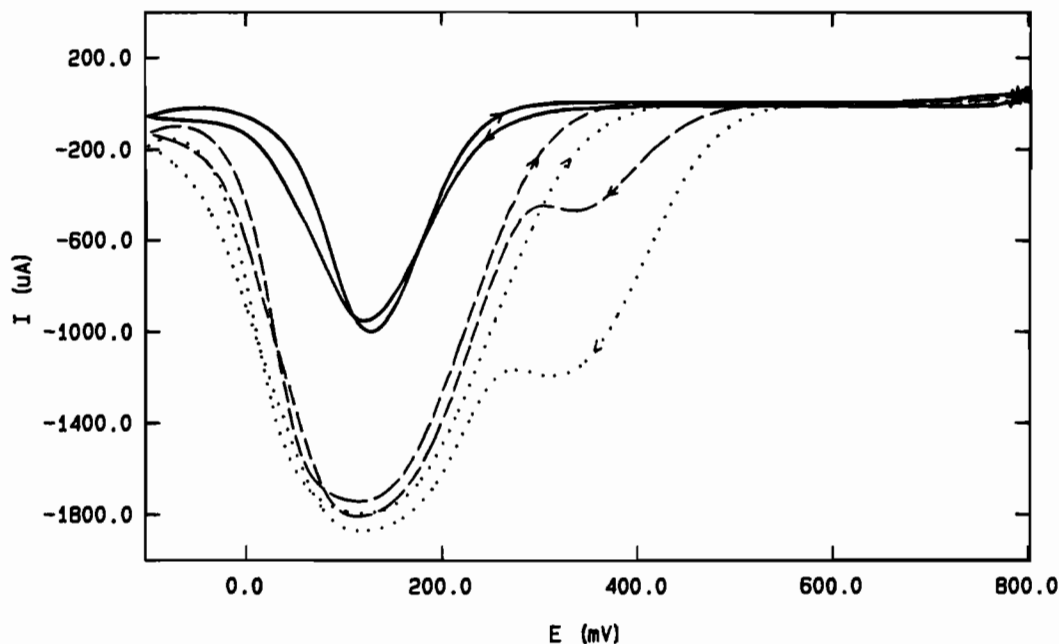


Figure 8. Rotating-disk cyclic voltammograms for the reduction of O_2 at a pyrolytic EPGE on which Ir(OEP)H is adsorbed: supporting electrolyte 0.1 M TFA saturated with O_2 ; scan rate 100 mV/s; rotation rate 1600 rpm. The solid line shows the result when the amount of Ir(OEP)H applied to the EPGE is ca. 1.2×10^{-10} mol cm^{-2} , the dashed line that at ca. 3.5×10^{-10} mol cm^{-2} , and the dotted line that at ca. 6.5×10^{-10} mol cm^{-2} .

$Ir_2DPA(TPP)(H)_2$, and $Ir_2DPA(TMP)(H)_2$ were originally conceived in order to determine if the catalysis proceeded through a monometallic or a bimetallic pathway. (For these molecules, it is believed that intramolecular metal-metal bond formation cannot occur.²⁰) If the catalysis involves two iridium centers acting in concert, then—as the metal centers in the cofacial diporphyrins are already held together in close proximity—one might expect that the electrocatalysis of dioxygen would be improved. Subsequent experiments showed this not to be the case. As can be seen from Table 3, $Ir_2DPA(H)_2$ and $Ir_2DPA(TPP)(H)_2$ do catalyze the four-electron reduction of dioxygen, but with less activity compared to their respective monomers. The cofacial diporphyrin, $Ir_2DPA(TMP)(H)_2$, like its monomer, Ir(TMP)(H), is an inactive catalyst.

The reduction of dioxygen catalyzed by dicobalt cofacial diporphyrins is dependent upon the geometry adopted by the cofacial diporphyrins and the cobalt-cobalt distance.^{3a} These two factors are determined by the length and type of linker(s) that is used to connect the two porphyrins in a cofacial manner. If the linker is not of the appropriate length, the dioxygen molecule will not be able to interact with the two metal centers simultaneously so that the reduction does not proceed all the way to water; instead, a two-electron reduction to hydrogen peroxide occurs. In the present study, the linker used for all the cofacial diporphyrins is an anthracene bridge. In earlier studies, Co_2DPA , the bis(cobalt) analog of $Ir_2DPA(H)_2$, was found to be an effective four-electron catalyst for dioxygen reduction.^{3d,f} If indeed the iridium catalysis also proceeds through a bimetallic pathway, we infer that the metal-metal distance and geometric requirements are met (at least for the $Ir_2DPA(H)_2$ case). For $Ir_2DPA(TPP)(H)_2$ and $Ir_2DPA(TMP)(H)_2$, we now believe that the increased steric demands of the porphyrins may not allow bimetallic activation of dioxygen.

Regardless, the results obtained for $Ir_2DPA(H)_2$ suggest that the four-electron reduction of dioxygen catalyzed by iridium porphyrins proceeds via a monometallic rather than a bimetallic pathway.

Catalyzed Dioxygen Reduction by Cofacial Bis(alkyliridium) Diporphyrins and Cofacial Mononickel Mono(alkyliridium) Diporphyrins. At this point, a number of questions still remain: (1) Does the catalysis proceed by a monometallic or bimetallic pathway or both? (2) Does the graphite provide axial ligation to the iridium metal center and is such axial ligation necessary for dioxygen reduction? (3) Are the R groups of the Ir(III) porphyrins stable during the course of the catalysis? To address these issues, a number of mono- and diiridium cofacial diporphyrin mono- and dialkyls were synthesized. All of these metalloporphyrins were produced as a mixture of regioisomers which were separated and tested individually for catalytic activity.

Charts 1 and 2 illustrate the combinations of hypothetical requirements for catalysis, and the expected catalyst behavior based solely on these requirements. Specifically, monometallic and bimetallic pathways are considered; necessity of axial ligation from the graphite surface and organometallic bond stability are included for each case.

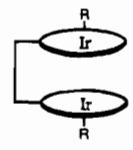
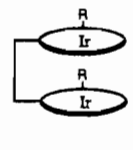
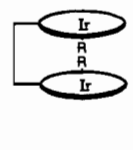
Experimentally it was found that the Ni(Ir)DPA(R)-in isomer (R = CH_3 or C_2H_5) is an active four-electron catalyst after positive conditioning but the out isomer fails to become activated even after conditioning (Table 4). The $Ir_2DPA(R)_2$ -in/out isomer (R = CH_3 or C_2H_5) catalyzes the reduction of dioxygen to water (after positive conditioning) whereas the out/out isomer does not. The Ni(Ir)DPA(R)-in isomers (R = CH_3 or C_2H_5) can also become active catalysts after negative conditioning (-2 V). Recall that this behavior is not seen for the Ir(OEP) CH_3 and Ir(OEP) C_2H_5 cases. Noteworthy are the studies of Kadish et al., who found that some Ni(I) porphyrin complexes catalyze the reduction of methyl iodide.²¹ Thus we believe that, in these cases, the nickel porphyrin in the cofacial diporphyrins becomes reduced at the negative potentials to form Ni(I). This complex

(19) (a) Collman, J. P.; Wagenknecht, P. S.; Hembre, R. T.; Lewis, N. S. *J. Am. Chem. Soc.* **1990**, *112*, 1294–1295. (b) Collman, J. P.; Wagenknecht, P. S.; Hutchison, J. E.; Lewis, N. S.; Lopez, M. A.; Guillard, R.; L'Her, M.; Bothner-By, A. A.; Mishra, P. K. *J. Am. Chem. Soc.* **1992**, *114*, 5654–5664.

(20) Collman, J. P.; Kim, K.; Garner, J. M. *J. Chem. Soc., Chem. Commun.* **1986**, 1711–1713.

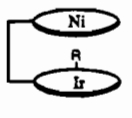
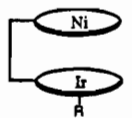
(21) Kadish, K. M.; Franzen, M. M.; Han, B. C.; Araullo-McAdams, C.; Sazou, D. *Inorg. Chem.* **1992**, *31*, 4399–4403.

Chart 1. Cofacial Bis(alkyliridium) Diporphyrin Cases^a

combinations of catalysis requirements			
Mono-metallic	Expected four electron catalyst of dioxygen reduction?		
R stays on Axial ligation	No	No	No
R stays on No axial ligation	Yes	Yes	Yes
R comes off Axial ligation	No	Yes	Yes
R comes off No axial ligation	Yes	Yes	Yes
Bi-metallic			
R stays on Axial ligation	No	No	No
R stays on No axial ligation	Yes	Yes	Yes
R comes off Axial ligation	No	No	No
R comes off No axial ligation	Yes	Yes	Yes

^a Note: "Axial ligation" refers to that from the electrode surface.

Chart 2. Cofacial Mononickel Mono(alkyliridium) Diporphyrin Cases^a

combinations of catalysis requirements		
Mono-metallic	Expected four electron catalyst of dioxygen reduction?	
R stays on Axial ligation	No	No
R stays on No axial ligation	Yes	Yes
R comes off Axial ligation	Yes	No
R comes off No axial ligation	Yes	Yes
Bi-metallic		
R stays on Axial ligation	No	No
R stays on No axial ligation	Yes	No
R comes off Axial ligation	No	No
R comes off No axial ligation	Yes	Yes

^a Note: "Axial ligation" refers to that from the electrode surface.

may somehow assist in the cleavage of the iridium-carbon bond to yield the active Ir(II) species.

These results indicate that the dioxygen reduction by iridium porphyrins occurs via a monometallic pathway and requires

interaction with the graphite surface (probably in the form of axial ligation to the iridium metal center) and that the R group is liberated to create a vacant coordination site for the dioxygen molecule. Ir₂DPA(H)₂ and Ir₂DPA(TPP)(H)₂ are worse catalysts compared to their monomers as they exist as a mixture of regioisomers and only the in/out and the in/in isomers can be active. The out/out isomers cannot catalyze the reduction of dioxygen to water.

Proposed Mechanisms for Dioxygen Reduction by Iridium Porphyrins. Schemes 2–5 show the proposed mechanisms for the dioxygen reduction by iridium porphyrins based upon the results that have been obtained.

Ir(OEP)H (Scheme 2) is apparently first oxidized by one electron, resulting in the loss of a proton to form the Ir(II) center. This active iridium(II) center should subsequently bind dioxygen and catalyze its four-electron reduction to water. This catalyst begins to lose its catalytic activity when it is scanned to a potential < 0 V, apparently because the Ir(II) becomes reduced to Ir(I). This is then protonated to re-form Ir(OEP)H. The nature of the intermediates in the catalytic cycle is uncertain. It is expected that Ir(II) would form a monohapto complex of O₂, formally Ir^{III}O₂⁻. The next expected complex in the reaction cycle, Ir^{III}OOH, is apparently not an intermediate. When Ir(OEP)OOH was prepared independently, it did not become an active catalyst until it was conditioned at reducing potentials.

The Ir(OEP)R systems (R = alkyl or aryl) have to be conditioned at positive potentials first in order for the iridium-carbon bond to undergo heterolysis to form an Ir(III) center and a carbon radical (Scheme 3). Axial ligation from the graphite surface is essential for this process to occur. Precedence for this can be found in the experiments of Kadish et al., who performed solution electrochemistry with Ir(OEP)-*n*-Pr.²² Their results indicate that the iridium-carbon bond is strong and will break only when there is a good π-acceptor (eg PPh₃ or P(OEt)₃) coordinated to the iridium metal. The Ir(III) is then reduced to Ir(II) during the voltammetric scan. This Ir(II) would then reduce dioxygen as shown in Scheme 2.

Ir(OEP)I and Ir(OEP)OOH (as mentioned above) must first be reduced at a negative potential in order to break the axial bond. Again, this generates the Ir(II) center (Scheme 4).

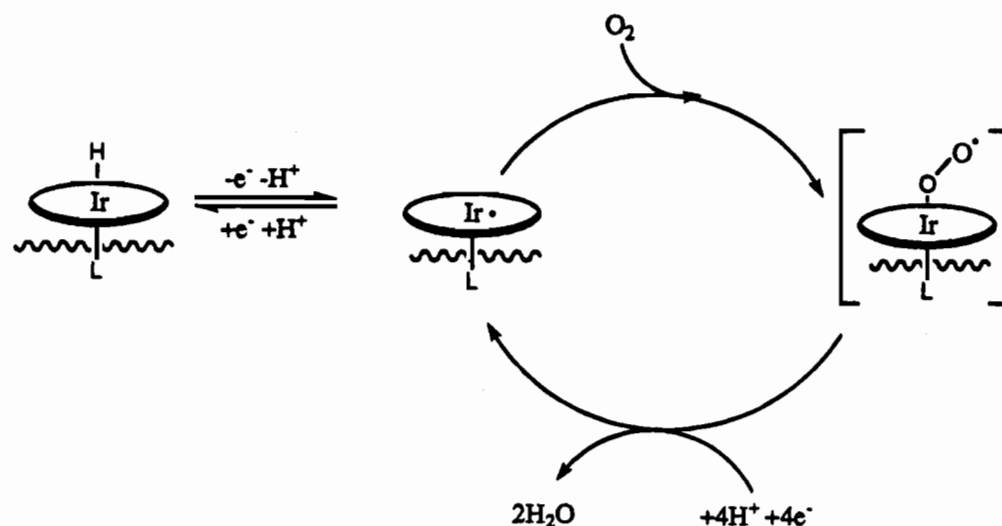
Scheme 5 illustrates the proposed mechanism by which the Ir(monomer)H catalyzes dioxygen reduction. The Ir(monomer)H porphyrins should be reduced at a negative potential to form [Ir(monomer)H]⁻. Subsequent protonation occurs, forming an iridium-dihydrogen complex. The dihydrogen would then be released and the resulting Ir(II) center reduced to Ir(I) at such a negative potential. As more positive potentials are reached (~0 V), Ir(II) is generated, and as before this would bind dioxygen and catalyze its reduction. At more positive potentials (> +0.4 V), the reducing current dies as the overpotential limit is reached. Ir(TMP)H and Ir(TMTMP)H are not active catalysts because they are sterically hindered, thus preventing the necessary axial ligation from the graphite surface to the iridium metal.

Conclusion

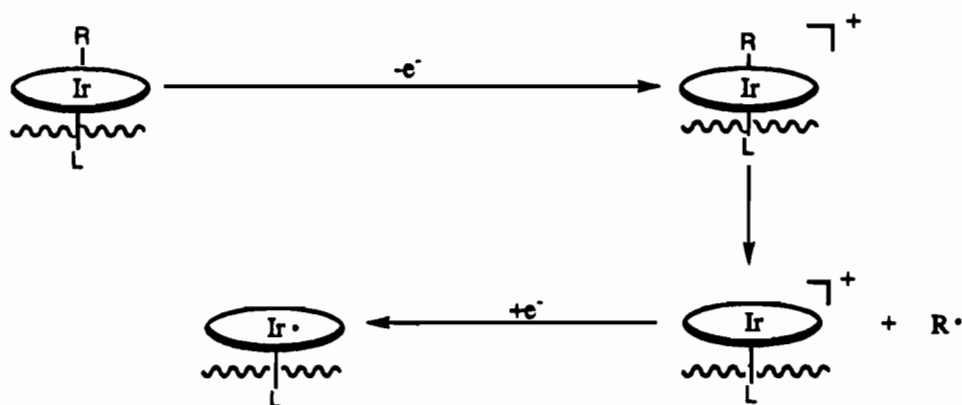
We have synthesized a family of iridium porphyrins which catalyzes the four-electron reduction of dioxygen to water on EPGE. We believe that the active catalyst is a surface-ligated Ir(II) center, not the dimer as previously conjectured. For the Ir(OEP) alkyl and aryl porphyrins, the active Ir(II) center is formed upon positive conditioning, as the iridium-carbon bond breaks when the porphyrin is oxidized. This bond cleavage is

(22) Kadish, K. M.; Cornillon, J.-L.; Mitaine, P.; Deng, Y. J.; Korp, J. D. *Inorg. Chem.* **1989**, *28*, 2534–2542.

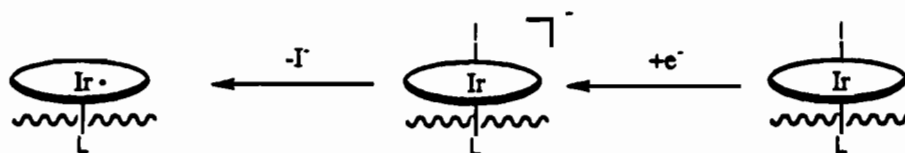
Scheme 2



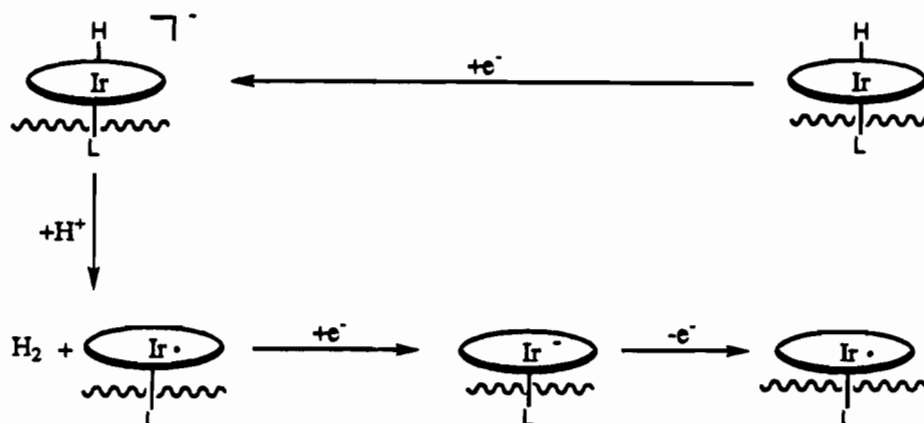
Scheme 3



Scheme 4



Scheme 5



assisted by axial ligation from the graphite surface. In the absence of interaction with the ligands present on the EPGE (as in the case of Ni(Ir)DPA(R)-out and Ir₂DPA(R)₂-out/out), the iridium-carbon bond is not cleaved upon porphyrin oxidation; the active Ir(II) center is not formed and thus no

dioxygen reduction occurs. Once an Ir(II) center is formed, it will interact with dioxygen and reduce it in a monometallic fashion.

For the other monomeric iridium porphyrins (Ir(TPP)H, Ir(TTP)H, and Ir(TnPP)H), their porphyrin-based reduction

potentials are higher than that of Ir(OEP)H. Thus we believe that the Ir(II) center is generated after reduction at a negative potential, followed by protonation and loss of dihydrogen. The formation of this active Ir(II) center is again dependent upon the presence of axial ligation from the EPGE. This follows from the fact that Ir(TMP)H and Ir(TMTMP)H are inactive catalysts—seemingly because their steric demands prevent the necessary axial ligand from the EPGE from interacting with the iridium center.

Experimental Section

Reagents and Solvents. All solvents and reagents were of reagent grade quality and were purchased commercially and used without further purification, unless otherwise noted. All the solvents used in the inert-atmosphere box were purified by literature methods.²³ NMR solvents (C₆D₆) for drybox use were vacuum-transferred from benzophenone ketyl. Water used for electrochemistry was purified by passing it through a Barnstead Nanopure purification train.

[Ir(COD)Cl]₂,²⁴ Ir(OEP)(CO)(Cl),⁹ Ir(OEP)H,⁹ Ir(OEP)CH₃,⁹ Ir(OEP)C₂H₅,⁹ Ir(OEP)CH₂Ph,¹⁰ Ir(OEP)I,⁹ Ir(OEP)OOH,⁶ Ir(TTP)(CO)(Cl),⁶ Ir(TPP)(CO)(Cl),²⁵ Ir(TTP)H,⁶ H₂TPP,²⁶ H₂TMP,²⁶ H₂TnPP,²⁷ H₂TMTMP,²⁸ H₄DPA,²⁹ H₄DPA(TMP),³⁰ and H₂ZnDPA^{3f} were synthesized according to literature procedures.

Physical and Spectroscopic Methods. All manipulations of oxygen and water-sensitive compounds were performed in a Vacuum/Atmosphere Co. nitrogen atmosphere drybox (O₂ ≤ 2 ppm). Oxygen levels were monitored with an AO 316-C trace oxygen analyzer. ¹H NMR spectra were obtained with a Nicolet NMC 300-MHz or a Varian XL 400-MHz spectrometer. UV/vis spectra were obtained with a Hewlett Packard 8450A diode array spectrometer. Mass spectra were done by the Mass Spectrometry Facility of the University of California at San Francisco. Infrared spectra were obtained with KBr pellet samples using an IBM 98FT-IR instrument. Elemental analyses were performed by Midwest Microlab.

The disk electrode and the ring-disk electrode were obtained from Pine Instrument Co., Grove City, PA. Rotating-disk voltammeteries were performed with a computer-controlled PAR 273A potentiostat/galvanostat. Rotating ring-disk voltammeteries were performed with a Model RDE 3 potentiostat (Pine Instrument Co.) using an ASR rotator (Pine Instrument Co.) and an HP 7046B X-Y recorder. The edge plane pyrolytic graphite electrodes were polished with No. 400 or No. 600 SiC paper, sonicated in deionized water for 10 s, rinsed with deionized water, and dried. Adsorption of the iridium porphyrins was performed in the inert-atmosphere box. A solution of the compound in benzene was syringed onto the electrode surface and allowed to evaporate. Depending on the experiment, the electrode may or may not have been rinsed with benzene. The experimental collection efficiency of the ring-disk electrode was 8% at 1600 rpm after the platinum ring had been treated.³¹ All potentials were measured vs a saturated calomel electrode (SCE). The electrolyte used in these studies was 0.1 M trifluoroacetic acid (aqueous) (TFA).

Syntheses. H₄DPA(TPP). This compound was synthesized in a stepwise fashion according to published literature procedures with slight modifications.³⁰

The first porphyrin condensation was performed with 1-(1,3-dithiacyclohex-2-yl)-8-formylanthracene, pyrrole, and benzaldehyde (in a stoichiometry of 1:13:12). Partial isolation of the desired product was achieved using a plug of silica (1:3 = CH₂Cl₂:hexanes). The major byproduct (H₂TPP) was eluted first. The product—the protected monoporphyrin—was eluted with 2:1 = CH₂Cl₂:hexanes as the next major band. Upon aldehyde deprotection, the reaction mixture was washed with aqueous sodium carbonate and purified by chromatography (silica, 1:1 = CH₂Cl₂:hexanes): yield 240 mg (35% based on the bridge); ¹H NMR (CDCl₃) δ 9.47 (s, 1H, anthracene or -CHO), 9.13 (s, 1H, anthracene or -CHO), 8.82 (m, 5H, H_β and anthracene or -CHO), 8.70 (d, 2H, H_β), 8.55 (d, 2H, H_β), 8.47 (d, 1H, anthracene), 8.3–7.5 (m, 20H, anthracene and phenyl), -2.55 (s, 2H, -NH); UV/vis (CH₂Cl₂) λ_{max} 422 (Soret), 514, 548, 592, 648 nm.

The second Lindsey condensation proceeded as described above, using 1:13:12 of the above monoporphyrin monoaldehyde, pyrrole, and benzaldehyde. The reaction mixture was partially purified with a silica plug (1:1 = CH₂Cl₂:hexanes). H₂TPP was eluted as the first major band. The product was eluted with CH₂Cl₂ as the second major band. This was then further purified on a silica column (1:1 = CH₂Cl₂:hexanes): yield 134 mg (33% based on the bridge porphyrin); ¹H NMR (CDCl₃) δ 9.09 (s, 1H, anthracene), 8.53 (d, 2H, anthracene), 8.41 (d, 4H, H_β), 8.34 (s, 1H, anthracene), 8.32 (d, 4H, H_β), 8.23 (d, 4H, H_β), 8.17 (d, 4H, H_β), 7.9–7 (m, 34H, anthracene and phenyl), -3.81 (s, 4H, -NH); UV/vis (CH₂Cl₂) λ_{max} 412 (Soret), 518, 552, 592, 648 nm; MS *m/e* 1252 (cluster, M⁺). Anal. Calc for C₉₀N₈H₅₈H₂O: C, 85.15; H, 4.76; N, 8.83. Found: C, 84.88; H, 4.89; N, 8.60.

Ir(TnPP)(CO)(Cl), Ir(TMP)(CO)(Cl), Ir(TMTMP)(CO)(Cl), Ir₂DPA(TPP)(CO)₂(Cl)₂, Ir₂DPA(TMP)(CO)₂(Cl)₂, Ir₂DPA(CO)₂(Cl)₂, Ir(OEP)-CH(CH₃)₂, Ir(OEP)Ph, Ir(OEP)C₆H₅(CH₃)₂, and Ir(OEP)C₆H₅(CF₃)₂ were synthesized using the procedures of Ogoshi et al.⁹ with slight modifications.

Ir(TnPP)(CO)(Cl). H₂TnPP (40 mg) and [Ir(COD)Cl]₂ (112 mg) were dissolved in 50 mL of *o*-xylene. The solution was purged with nitrogen for 10 min and refluxed under a nitrogen atmosphere for 20 h. The solvent was removed by vacuum distillation and the solid chromatographed on silica with dichloromethane. The product was eluted as the second major band (pink) in 40% yield: ¹H NMR (CDCl₃) δ 9.55 (s, 8H, H_β), 4.93 (t, 8H, -CH₂CH₂CH₃), 2.65 (m, 8H, -CH₂CH₂-CH₃), 1.38 (t, 12H, -CH₂CH₂CH₃); UV/vis (CH₂Cl₂) λ_{max} 314, 422 (Soret), 502, 538, 572 nm; MS *m/e* 732 (cluster, M⁺); IR (KBr) 2054 cm⁻¹, ν(CO). Anal. Calc for IrC₃₃N₄H₃₆OCl: C, 54.12; H, 4.95; N, 7.65; Cl, 4.84. Found: C, 53.95; H, 4.89; N, 7.52; Cl, 5.07.

Ir(TMP)(CO)(Cl). H₂TMP (50 mg) and [Ir(COD)Cl]₂ (300 mg) were refluxed in 35 mL of *o*-xylene for 36 h under nitrogen. The solvent was removed by vacuum distillation and the solid chromatographed on silica. The product was eluted as the second band (red) with 2:1 = CH₂Cl₂:hexanes in 60% yield: ¹H NMR (CDCl₃) δ 8.64 (s, 8H, H_β), 7.26 (s, 4H, H_m), 7.24 (s, 4H, H_m, buried under solvent peak), 2.60 (s, 12H, *p*-CH₃, mesityl), 1.90 (s, 12H, *o*-CH₃, mesityl), 1.80 (s, 12H, *o*-CH₃, mesityl); UV/vis (CH₂Cl₂) λ_{max} 316, 422 (Soret), 496, 532, 546 nm; MS *m/e* 1036 (cluster, M⁺); IR (KBr) 2045 cm⁻¹, ν(CO). Anal. Calc for IrC₃₇N₄H₅₂OCl: C, 66.04; H, 5.06; N, 5.40; Cl, 3.42. Found: C, 66.21; H, 5.09; N, 5.30; Cl, 3.63.

Ir(TMTMP)(CO)(Cl). H₂TMTMP (20 mg) and [Ir(COD)Cl]₂ (112 mg) were refluxed in 20 mL of *o*-xylene under a nitrogen atmosphere for 20 h. After the solvent had been removed, the solid was chromatographed on silica. The product was eluted as the second band (pink) with 1:1 = CH₂Cl₂:hexanes in 40% yield: ¹H NMR (CDCl₃) δ 9.80 (s, 4H, meso), 7.29 (s, 8H, H_m), 3.28 (s, 12H, -CH₃), 2.58 (s, 12H, *p*-CH₃, mesityl), 2.22 (s, 12H, *o*-CH₃, mesityl), 2.16 (s, 12H, *o*-CH₃, mesityl); UV/vis (CH₂Cl₂) λ_{max} 346, 406 (Soret), 518, 550 nm; MS *m/e* 1091 (cluster, M⁺ + 1); IR (KBr) 2046 cm⁻¹, ν(CO). Anal. Calc for IrC₆₁N₄H₆₀OCl: C, 67.04; H, 5.53; N, 5.13. Found: C, 67.04; H, 5.64; N, 4.99.

Ir₂DPA(TPP)(CO)₂(Cl)₂. H₄DPA(TPP) (10 mg) and [Ir(COD)Cl]₂ (22 mg) were refluxed in 12 mL of *o*-xylene under nitrogen for 16 h. The solvent was removed, and the reaction mixture was separated on preparative TLC (silica, 3:1 = CH₂Cl₂:hexanes). Two major orange-red bands (fifth, 18% yield; sixth, 22% yield) were collected. Fifth band: ¹H NMR (CDCl₃) δ 9.13–6.86 (anthracene, H_β and H_{phenyl}); UV/vis (CH₂Cl₂) λ_{max} 322, 414 (Soret), 532, 566 nm; MS *m/e* 1758 (cluster,

- (23) Perrin, D. D.; Armarego, W. L. F.; Perrin, D. R. *Purification of Laboratory Chemicals*, 2nd ed.; Pergamon Press Ltd.: London, 1980.
- (24) Herde, J. L.; Lambert, J. C.; Senoff, C. V. *Inorg. Synth.* **1974**, *15*, 18–19.
- (25) Swistak, C.; Cornillon, J.-L.; Anderson, J. E.; Kadish, K. M. *Organometallics* **1987**, *6*, 2146–2150.
- (26) Lindsey, J. S.; Wagner, R. W. *J. Org. Chem.* **1989**, *54*, 828–836.
- (27) Lindsey, J. S.; Schreiman, I. C.; Hsu, H. C.; Kearney, P. C.; Marguerettaz, A. M. *J. Org. Chem.* **1987**, *52*, 827–836.
- (28) Ono, N.; Kawamura, H.; Bougauchi, M.; Maruyama, K. *Tetrahedron* **1990**, *46*, 7483–7496.
- (29) (a) Chang, C. K.; Abdalmuhdi, I. *J. Org. Chem.* **1983**, *48*, 5388–5390. (b) Guilard, R.; Lopez, M. A.; Tabard, A.; Richard, P.; Lecomte, C.; Brandes, S.; Hutchison, J. E.; Collman, J. P. *J. Am. Chem. Soc.* **1992**, *114*, 9877–9889.
- (30) Collman, J. P.; Tyvoll, D. A.; Chng, L. L.; Fish, H. T. Submitted for publication.
- (31) Ni, C.-L.; Abdalmuhdi, I.; Chang, C. K.; Anson, F. C. *J. Phys. Chem.* **1987**, *91*, 1158–1166.

M⁺). Sixth band: ¹H NMR (CDCl₃) δ 9.16 (s, 1H, anthracene), 8.71 (s, 1H, anthracene), 8.60 (d, 4H, H_β), 8.58 (d, 2H, anthracene), 8.47 (d, 4H, H_β), 8.41 (d, 4H, H_β), 8.28 (d, 4H, H_β), 8.1–6.8 (m, 34H, phenyl and anthracene); UV/vis (CH₂Cl₂) λ_{max} 322, 414 (Soret), 532, 566 nm; MS *m/e* 1759 (cluster, M⁺ + 1).

Ir₂DPA(TMP)(CO)₂(Cl)₂. H₄DPA(TMP) (10 mg) and [Ir(COD)-Cl]₂ (100 mg) were refluxed in 40 mL of *o*-xylene under nitrogen for 29 h. The solvent was removed and the reaction mixture was separated on TLC (silica, 3:1 = CH₂Cl₂:hexanes). The second (20% yield) and third (15% yield) bands (orange-red) were collected. Second band: ¹H NMR (CDCl₃) δ 9.10 (s, 1H, anthracene), 8.53 (d, 2H, anthracene), 8.29 (d, 4H, H_β), 8.24 (d, 4H, H_β), 8.16 (d, 4H, H_β), 8.03 (d, 4H, H_β), 7.8 (m, 5H, anthracene), 7.16 (s, 2H, H_{mesityl}), 7.10 (s, 2H, H_{mesityl}), 7.07 (s, 4H, H_{mesityl}), 7.01 (s, 4H, H_{mesityl}), 2.55 (s, 6H, *p*-CH₃, mesityl), 2.52 (s, 12H, *p*-CH₃, mesityl), 1.70 (s, 6H, *o*-CH₃, mesityl), 1.24 (s, 12H, *o*-CH₃, mesityl), 1.08 (s, 6H, *o*-CH₃, mesityl), 1.05 (s, 12H, *o*-CH₃, mesityl); UV/vis (CH₂Cl₂) λ_{max} 318, 418 (Soret), 534, 568 nm; MS *m/e* 2011 (cluster, M⁺). Third band: ¹H NMR (CDCl₃) δ 9.2–6.9 (36H, anthracene, H_β and H_{mesityl}), 2.5–1 (54H, -CH₃, mesityl); UV/vis (CH₂Cl₂) λ_{max} 318, 418 (Soret), 534, 568 nm; MS *m/e* 2011 (cluster, M⁺).

Ir₂DPA(CO)₂(Cl)₂. H₄DPA (20 mg) and [Ir(COD)Cl]₂ (47 mg) were refluxed in 30 mL of *o*-xylene under nitrogen for 20 h. The solvent was removed and the solid was chromatographed (silica, CH₂Cl₂). The third (18% yield) and the fourth bands (24% yield) (pinkish-red) were isolated. Third band: ¹H NMR (CDCl₃) δ 9.7–6.8 (14H, meso and anthracene), 3.9–3.3 (16H, -CH₂CH₃), 3.26–2.09 (24H, -CH₃), 1.7–1.2 (24H, -CH₂CH₃); UV/vis (CH₂Cl₂) λ_{max} 346, 402 (Soret), 520, 552; MS *m/e* 1638 (cluster, M⁺). Fourth band: ¹H NMR (CDCl₃) δ 9.77 (s, 2H, meso), 9.45 (s, 4H, meso), 9.19 (s, 1H, anthracene), 8.78 (s, 1H, anthracene), 8.62 (d, 2H, anthracene), 7.73 (t, 2H, anthracene), 7.37 (d, 2H, anthracene), 3.9–3.3 (m, 16H, -CH₂CH₃), 3.25 (s, 12H, -CH₃), 2.08 (s, 12H, -CH₃), 1.69 (t, 12H, -CH₂CH₃), 1.04 (t, 12H, -CH₂CH₃); UV/vis (CH₂Cl₂) λ_{max} 346, 400 (Soret), 520, 552 nm; MS *m/e* 1639 (cluster, M⁺ + 1).

Ir(OEP)CH(CH₃)₂. A 10 mg amount of Ir(OEP)(CO)(Cl) was dissolved in 20 mL of refluxing ethanol under nitrogen; 4 mg of NaBH₄ in 2 mL of 1 N NaOH was degassed and syringed in. This mixture was refluxed for 1 h. Then 20 μL of (CH₃)₂CHBr was degassed and syringed in and the resulting solution was refluxed for 4 h. The red solution was allowed to cool, and 30 mL of degassed deionized water was cannulated into the reaction mixture. The red precipitate formed was collected on a Celite pad and washed with deionized water. This was dried under vacuum and then taken into the inert-atmosphere box. The solid was dissolved in benzene, and the solution was filtered. The solvent was evaporated, and the residue was then purified by column chromatography (silica, 1:1 = benzene:hexanes). The product was eluted as the first red band in 80% yield: ¹H NMR (C₆D₆) δ 9.92 (s, 4H, meso), 3.94 (m, 16H, -CH₂CH₃), 1.89 (t, 24H, -CH₂CH₃), -4.53 (d, 6H, -CH(CH₃)₂, axial ligand), -4.56 (m, 1H, -CH(CH₃)₂, axial ligand); UV/vis (C₆H₆) λ_{max} 342, 388 (Soret), 498, 528 nm; MS *m/e* 768 (cluster, M⁺).

Ir(OEP)Ph. A 4 mg sample of lithium and 27 μL of bromobenzene were stirred vigorously in 4 mL of dry THF in the argon box for 2 h. The resulting brown solution was filtered, and the filtrate was added to a solution of Ir(OEP)(CO)(Cl) in 25 mL of THF. This mixture was refluxed for 5 h under an inert atmosphere. The solvent was then rotoevaporated, and the solid was chromatographed (silica, benzene). The first red band was collected. This was further purified on preparative TLC (silica, 1:3 = CH₂Cl₂:hexanes). The major reddish-pink band was collected (20% yield): ¹H NMR (C₆D₆) δ 10.03 (s, 4H, meso), 4.86 (t, 1H, *p*-H, phenyl ligand), 4.53 (t, 2H, *m*-H, phenyl ligand), 3.9 (m, 16H, -CH₂CH₃), 1.86 (t, 24H, -CH₂CH₃), 0.49 (d, 2H, *o*-H, phenyl ligand); UV/vis (C₆H₆) λ_{max} 336, 392 (Soret), 500, 530 nm; MS *m/e* 802 (cluster M⁺).

Ir(OEP)C₆H₃(CH₃)₂. This compound was synthesized in a manner similar to that for Ir(OEP)Ph. The organolithium reagent was generated with lithium and 5-bromo-*m*-xylene. The product was purified on preparative TLC (silica, 1:5 = CH₂Cl₂:hexanes): yield 18%; ¹H NMR (C₆D₆) δ 10.01 (s, 4H, meso), 4.52 (s, 1H, *p*-H, xylyl ligand), 3.89 (m, 16H, -CH₂CH₃), 1.87 (t, 24H, -CH₂CH₃), 0.60 (s, 6H, *m*-CH₃, xylyl

ligand), 0.29 (s, 2H, *o*-H, xylyl ligand); UV/vis (C₆H₆) λ_{max} 338, 392 (Soret), 502, 530 nm; MS *m/e* 831 (cluster, M⁺).

Ir(OEP)C₆H₃(CF₃)₂. This iridium porphyrin was synthesized by following the procedure for Ir(OEP)Ph. The organolithium reagent was obtained by stirring lithium and 3,5-bis(trifluoromethyl)bromobenzene in THF for 24 h. The product was purified on preparative TLC (silica, 1:3 = CH₂Cl₂:hexanes): yield 15%; ¹H NMR (C₆D₆) δ 10.09 (s, 4H, meso), 5.40 (s, 1H, *p*-H, axial ligand), 3.85 (m, 16H, -CH₂CH₃), 1.84 (t, 24H, -CH₂CH₃), 0.64 (s, 2H, *o*-H, axial ligand); UV/vis (C₆H₆) λ_{max} 328, 390 (Soret), 502, 532 nm; MS *m/e* 938 (cluster, M⁺).

[Ir(OEP)]₂. Ir(OEP)CH₂Ph (2 mg) was dissolved in dry C₆D₆ (0.5 mL) in an E-J Young NMR tube. The solution was frozen—pumped—thawed twice and then photolyzed with a mercury lamp. The tube was cooled by immersing it in an ice—water bath. The progress of the reaction was monitored using ¹H NMR. The ¹H NMR spectrum obtained was the same as that reported in the literature.^{10,11}

Ir(TnPP)H, Ir(TMP)(H), Ir(TMTMP)H, Ir₂DPA(TPP)(H)₂, Ir₂DPA(TMP)(H)₂, and Ir₂DPA(H)₂ were synthesized using the procedures of Ogoshi et al.⁹

Ir(TnPP)H: ¹H NMR (C₆D₆) δ 8.78 (s, 8H, H_β), 4.42 (t, 8H, -CH₂-CH₂CH₃), 2.40 (m, 8H, -CH₂CH₂CH₃), 1.23 (t, 12H, -CH₂CH₂CH₃), -56.90 (s, 1H, -H, axial ligand); UV/vis (C₆H₆) λ_{max} 326, 410 (Soret), 512 nm; MS *m/e* 669 (cluster, M⁺ - 1).

Ir(TMP)H: ¹H NMR (C₆D₆) δ 8.59 (s, 8H, H_β), 7.19 (s, 4H, H_m), 7.08 (s, 4H, H_m), 2.42 (s, 12H, *p*-CH₃, mesityl), 2.24 (s, 12H, *o*-CH₃, mesityl), 1.80 (s, 12H, *o*-CH₃, mesityl), -58.07 (s, 1H, -H, axial ligand); UV/vis (C₆H₆) λ_{max} 326, 406 (Soret), 504 nm; MS *m/e* 973 (cluster, M⁺ - 1).

Ir(TMTMP)H: ¹H NMR (C₆D₆) δ 9.79 (s, 4H, meso), 7.26 (s, 4H, H_m), 7.15 (s, 4H, H_m, buried under solvent peak), 3.04 (s, 12H, -CH₃), 2.4 (s, 24H, -CH₃, mesityl), 2.19 (s, 12H, -CH₃, mesityl), -57.81 (s, 1H, -H, axial ligand); UV/vis (C₆H₆) λ_{max} 334, 394 (Soret), 503, 530 nm; MS *m/e* 1029 (cluster, M⁺ - 1).

Ir₂DPA(TPP)(H)₂: ¹H NMR (C₆D₆) δ 9.3–6.8 (anthracene, H_β and H_{phenyl}), -57.82, -58.12, -59.37, -60.88 (s, -H, axial ligand); UV/vis (C₆H₆) λ_{max} 328, 406 (Soret), 512; MS *m/e* 1632 (cluster, M⁺ - 2).

Ir₂DPA(TMP)(H)₂: ¹H NMR (C₆D₆) δ 9.4–6.8 (anthracene, H_β and H_{mesityl}), 2.5–0.7 (s, 54H, -CH₃), -57.65, -58.10, -59.30, -60.65 (s, -H, axial ligand); UV/vis (C₆H₆) λ_{max} 328, 406 (Soret), 512 nm; MS *m/e* 1884 (cluster, M⁺ - 3).

Ir₂DPA(H)₂. The precipitated product was collected by filtration using Schlenk techniques: ¹H NMR (C₆D₆) δ 9.4–6.3 (anthracene and meso), 4.4–3.4 (-CH₂CH₃), 3.34 (-CH₃), 2.09 (-CH₃), 1–2 (-CH₂CH₃), -58.29, -62.72, -66.16 (s, -H, axial ligand); UV/vis (C₆H₆) λ_{max} 336, 380 (Soret), 505, 534; MS *m/e* 1512 (cluster, M⁺ - 2).

Ir₂DPA(CH₃)₂. Ir₂DPA(CO)₂(Cl)₂ (5 mg) was dissolved in 15 mL of refluxing ethanol under nitrogen, and 4 mg of NaBH₄ in 2 mL of 1 N NaOH was degassed and syringed in. The solution was refluxed for 1 h, 40 μL of degassed CH₃I was syringed in, and the solution was heated gently for 5 h. This was then cooled, and 30 mL of degassed deionized water was cannulated into the solution. The red precipitate was collected and chromatographed (silica, 1:1 = benzene:hexanes) to give a mixture of the regioisomers. The mixture was then separated on preparative TLC (silica, 1:4 = CH₂Cl₂:hexanes) to yield the out/out isomer as the first band (50%) and the in/out isomer as the last band (12%).

Ir₂DPA(CH₃)₂-out/out: ¹H NMR (C₆D₆) δ 9.19 (s, 4H, meso), 9.16 (s, 2H, meso), 8.82 (s, 1H, anthracene), 8.58 (s, 1H, anthracene), 8.36 (d, 2H, anthracene), 7.48 (t, 2H, anthracene), 7.40 (d, 2H, anthracene), 3.8–3.4 (m, 16H, -CH₂CH₃), 3.00 (s, 12H, -CH₃), 2.26 (s, 12H, -CH₃), 1.53 (t, 12H, -CH₂CH₃), 1.50 (t, 12H, -CH₂CH₃), -6.81 (s, 6H, -CH₃, axial ligand); UV/vis (C₆H₆) λ_{max} 338, 394 (Soret), 505, 532 nm; MS *m/e* 1543 (cluster, M⁺).

Ir₂DPA(CH₃)₂-in/out: ¹H NMR (C₆D₆) δ 9.29 (s, 1H, meso or anthracene), 9.13 (s, 3H, meso and anthracene), 9.08 (s, 1H, meso or anthracene), 8.86 (s, 2H, meso), 8.71 (s, 1H, meso or anthracene), 8.36 (d, 1H, anthracene), 8.29 (d, 1H, anthracene), 7.81 (d, 1H, anthracene), 7.60 (t, 1H, anthracene), 7.49 (t, 1H, anthracene), 7.44 (d, 1H, anthracene), 3.9–3.2 (m, 16H, -CH₂CH₃), 3.11 (s, 6H, -CH₃), 3.09 (s, 6H, -CH₃), 2.12 (s, 6H, -CH₃), 2.04 (s, 6H, -CH₃), 1.77 (t, 6H, -CH₂CH₃), 1.75 (t, 6H, -CH₂CH₃), 1.51 (t, 6H, -CH₂CH₃), 1.35 (t, 6H, -CH₂CH₃), -6.82 (s, 3H, -CH₃, axial ligand), -12.98 (s, 3H, -CH₃,

axial ligand); UV/vis (C_6H_6) λ_{max} 340, 390 (Soret), 503, 532 nm; MS *m/e* 1543 (cluster, M^+).

Ir₂DPA(C₂H₅)₂. This compound was synthesized in a fashion analogous to that above using ethyl iodide as the alkylating agent. The isomers were separated on preparative TLC (silica, 1:4 = CH_2Cl_2 :hexanes) to yield the out/out isomer as the first major band (46%) and the in/out isomer as the second major band (8%).

Ir₂DPA(C₂H₅)₂-out/out: ¹H NMR (C_6D_6) δ 9.16 (s, 4H, meso), 9.13 (s, 2H, meso), 8.83 (s, 1H, anthracene), 8.61 (s, 1H, anthracene), 8.37 (d, 2H, anthracene), 7.3 (m, 4H, anthracene), 3.8–3.4 (m, 16H, $-CH_2-CH_3$), 3.01 (s, 12H, $-CH_3$), 2.26 (s, 12H, $-CH_3$), 1.53 (m, 24H, $-CH_2CH_3$), -5.03 (t, 6H, $-CH_2CH_3$, axial ligand), -6.16 (q, 4H, $-CH_2-CH_3$, axial ligand); UV/vis (C_6H_6) λ_{max} 340, 392 (Soret), 502, 532 nm; MS *m/e* 1571 (cluster, M^+).

Ir₂DPA(C₂H₅)₂-in/out: ¹H NMR (C_6D_6) δ 9.21 (s, 1H, meso or anthracene), 9.18 (s, 2H, meso), 9.10 (s, 3H, meso and anthracene), 8.81 (s, 1H, meso or anthracene), 8.41 (d, 1H, anthracene), 8.41 (s, 1H, meso or anthracene), 8.33 (d, 1H, anthracene), 7.74 (d, 1H, anthracene), 7.61 (t, 1H, anthracene), 7.45 (t, 1H, anthracene), 7.15 (d, 1H, anthracene, buried under solvent peak), 3.8–3.4 (m, 16H, $-CH_2-CH_3$), 3.00 (s, 6H, $-CH_3$), 2.97 (s, 6H, $-CH_3$), 2.25 (s, 6H, $-CH_3$), 2.18 (s, 6H, $-CH_3$), 1.55 (t, 6H, $-CH_2CH_3$), 1.49 (m, 12H, $-CH_2CH_3$), 1.41 (t, 6H, $-CH_2CH_3$), -5.02 (t, 3H, $-CH_2CH_3$, axial ligand), -5.92 (q, 2H, $-CH_2CH_3$, axial ligand), -9.6 (m, 5H, $-CH_2CH_3$, axial ligand); UV/vis (C_6H_6) λ_{max} 342, 390 (Soret), 502, 530; MS *m/e* 1571 (cluster, M^+).

Ni(Zn)DPA. H_2ZnDPA (80 mg) was dissolved in 80 mL of $CHCl_3$. The solution was refluxed, and 80 mg of $Ni(OAc)_2 \cdot 4H_2O$ in MeOH was added. After 1 h and 15 min of reflux, the solution was cooled and the solvent evaporated. The red solid was then chromatographed (silica, CH_2Cl_2). The product was eluted as the first red band in 82% yield: ¹H NMR (C_6D_6) δ 9.55 (s, 1H, meso or anthracene), 9.21 (s, 1H, meso or anthracene), 8.90 (s, 2H, meso), 8.62 (s, 1H, meso or anthracene), 8.4–6.8 (7H, anthracene), 7.75 (s, 2H, meso), 4.2–3.2 (m, 16H, $-CH_2CH_3$), 2.83 (s, 6H, $-CH_3$), 2.79 (s, 6H, $-CH_3$), 2.14 (s, 6H, $-CH_3$), 1.80 (t, 6H, $-CH_2CH_3$), 1.70 (t, 6H, $-CH_2CH_3$), 1.64 (s, 6H, $-CH_3$), 1.46 (t, 6H, $-CH_2CH_3$), 1.14 (t, 6H, $-CH_2CH_3$); UV/vis (CH_2Cl_2) λ_{max} 392 (Soret), 538, 548, 562; MS *m/e* 1250 (cluster, $M^+ + 1$).

H₂NiDPA. $Ni(Zn)DPA$ (69 mg) was dissolved in 20 mL of CH_2Cl_2 , and 4 mL of 6 N HCl was added. The solution was stirred vigorously for 15 min. Aqueous Na_2CO_3 was then added to neutralize the solution, and this was stirred vigorously for 15 min. The organic layer was washed with water, dried, and evaporated to give the product in quantitative yield: ¹H NMR (C_6D_6) δ 9.55 (s, 1H, meso or anthracene), 9.31 (s, 1H, meso or anthracene), 8.75 (s, 2H, meso), 8.61 (s, 1H, meso or anthracene), 8.30 (d, 1H, anthracene), 8.16 (d, 1H, anthracene), 7.81 (d, 1H, anthracene), 7.77 (s, 2H, meso), 7.61 (s, 1H, meso or anthracene), 7.59 (dd, 1H, anthracene), 7.30 (dd, 1H, anthracene), 7.01 (d, 1H, anthracene), 4–2.4 (m, 16H, $-CH_2CH_3$), 2.72 (s, 6H, $-CH_3$), 2.67 (s, 6H, $-CH_3$), 2.07 (s, 6H, $-CH_3$), 1.76 (t, 6H, $-CH_2CH_3$), 1.71 (t, 6H, $-CH_2CH_3$), 1.66 (s, 6H, $-CH_3$), 1.31 (t, 6H, $-CH_2CH_3$), 0.99 (t, 6H, $-CH_2CH_3$), -4.20 (s, 1H, $-NH$), -4.35 (s, 1H, $-NH$); UV/vis (CH_2Cl_2) λ_{max} 392 (Soret), 514, 564, 632 nm; MS *m/e* 1188 (cluster, $M^+ + 1$).

Ni(Ir)DPA(CO)(Cl). H_2NiDPA (66 mg) and $[Ir(COD)Cl]_2$ (75 mg) were dissolved in 50 mL of *o*-xylene. The solution was refluxed under nitrogen for 15 h, the solvent was removed, and the solid was chromatographed (silica, CH_2Cl_2). The product was eluted as the second (red) band; it contained both regioisomers: yield 40%; ¹H NMR (C_6D_6) δ 9.74 (s, 2H, meso), 9.64 (s, 1H, meso or anthracene), 8.89 (s, 1H, meso or anthracene), 8.76 (s, 3H, meso and anthracene), 8.43 (s, 1H, meso or anthracene), 8.36 (d, 1H, anthracene), 8.24 (d, 1H, anthracene), 7.49 (dd, 1H, anthracene), 7.38 (d, 1H, anthracene), 7.32 (dd, 1H, anthracene), 6.89 (d, 1H, anthracene), 3.9–3.2 (m, 16H, $-CH_2-CH_3$), 3.02 (s, 6H, $-CH_3$), 2.70 (s, 6H, $-CH_3$), 2.34 (s, 6H, $-CH_3$), 2.00 (s, 6H, $-CH_3$), 1.51 (t, 6H, $-CH_2CH_3$), 1.46 (t, 6H, $-CH_2CH_3$), 1.27 (t, 6H, $-CH_2CH_3$), 1.20 (t, 6H, $-CH_2CH_3$); UV/vis (CH_2Cl_2) λ_{max} 346, 394 (Soret), 520, 552; MS *m/e* 1440 (cluster, M^+).

Ni(Ir)DPA(CH₃). This porphyrin was synthesized in a manner similar to that used for $Ir_2DPA(CH_3)_2$. The in and the out isomers were separated on preparative TLC (silica, 1:3.5 = CH_2Cl_2 :hexanes). The first band was the out isomer (60%), and the second band was the in isomer (10%).

Ni(Ir)DPA(CH₃)-out: ¹H NMR (C_6D_6) δ 9.36 (s, 1H, meso or anthracene), 9.14 (s, 1H, meso or anthracene), 8.84 (s, 2H, meso), 8.68 (s, 1H, meso or anthracene), 8.31 (d, 1H, anthracene), 8.21 (t, 1H, anthracene), 8.07 (s, 2H, meso), 7.63 (d, 1H, anthracene), 7.53 (t, 1H, anthracene), 7.3 (m, 2H, anthracene), 7.06 (d, 1H, anthracene), 3.8–3.2 (m, 16H, $-CH_2CH_3$), 2.83 (s, 6H, $-CH_3$), 2.80 (s, 6H, $-CH_3$), 2.18 (s, 6H, $-CH_3$), 1.86 (s, 6H, $-CH_3$), 1.68 (t, 6H, $-CH_2CH_3$), 1.54 (t, 6H, $-CH_2CH_3$), 1.45 (t, 6H, $-CH_2CH_3$), 1.25 (t, 6H, $-CH_2CH_3$), -6.76 (s, 3H, $-CH_3$, axial ligand); UV/vis (C_6H_6) λ_{max} 342, 396 (Soret), 534, 560 nm; MS *m/e* 1393 (cluster, M^+).

Ni(Ir)DPA(CH₃)-in: ¹H NMR (C_6D_6) δ 9.18 (s, 2H, meso), 9.09 (s, 1H, meso or anthracene), 8.82 (s, 1H, meso or anthracene), 8.75 (s, 2H, meso), 8.73 (s, 1H, meso or anthracene), 8.39 (d, 1H, anthracene), 8.23 (d, 1H, anthracene), 7.92 (s, 1H, meso or anthracene), 7.88 (d, 1H, anthracene), 7.66 (t, 1H, anthracene), 7.15 (t, 1H, anthracene, buried under solvent peak), 6.99 (d, 1H, anthracene), 3.8–3.2 (m, 16H, $-CH_2-CH_3$), 3.11 (s, 6H, $-CH_3$), 2.81 (s, 6H, $-CH_3$), 2.24 (s, 6H, $-CH_3$), 1.92 (s, 6H, $-CH_3$), 1.58 (t, 6H, $-CH_2CH_3$), 1.52 (t, 6H, $-CH_2CH_3$), 1.39 (t, 6H, $-CH_2CH_3$), 1.28 (t, 6H, $-CH_2CH_3$), -10.01 (s, 3H, $-CH_3$, axial ligand); UV/vis (C_6H_6) λ_{max} 342, 396 (Soret), 532, 560 nm; MS *m/e* 1393 (cluster, M^+).

Ni(Ir)DPA(C₂H₅). This compound was synthesized in a manner similar to that used for $Ir_2DPA(C_2H_5)_2$. The regioisomers were separated on preparative TLC (silica, 1:3.5 = CH_2Cl_2 :hexanes). The out isomer appeared as the first (red) band (58%), and the in isomer appeared as the second (red) band (10%).

Ni(Ir)DPA(C₂H₅)-out: ¹H NMR (C_6D_6) δ 9.35 (s, 1H, meso or anthracene), 9.16 (s, 1H, meso or anthracene), 8.76 (s, 2H, meso), 8.67 (s, 1H, meso or anthracene), 8.31 (d, 1H, anthracene), 8.22 (d, 1H, anthracene), 8.13 (s, 1H, meso or anthracene), 7.98 (s, 2H, meso), 7.67 (d, 1H, anthracene), 7.54 (t, 1H, anthracene), 7.3 (m, 1H, anthracene), 7.02 (d, 1H, anthracene), 3.8–2.8 (m, 16H, $-CH_2CH_3$), 2.81 (s, 6H, $-CH_3$), 2.80 (s, 6H, $-CH_3$), 2.16 (s, 6H, $-CH_3$), 1.84 (s, 6H, $-CH_3$), 1.71 (t, 6H, $-CH_2CH_3$), 1.56 (t, 6H, $-CH_2CH_3$), 1.44 (t, 6H, $-CH_2CH_3$), 1.24 (t, 6H, $-CH_2CH_3$), -5.10 (t, 3H, $-CH_2CH_3$, axial ligand), -6.10 (q, 2H, $-CH_2CH_3$, axial ligand); UV/vis (C_6H_6) λ_{max} 342, 394 (Soret), 532, 560; MS *m/e* 1406 (cluster, $M^+ - 1$).

Ni(Ir)DPA(C₂H₅)-in: ¹H NMR (C_6D_6) δ 9.33 (s, 2H, meso), 9.20 (s, 1H, meso or anthracene), 8.98 (s, 1H, meso or anthracene), 8.83 (s, 2H, meso), 8.77 (s, 1H, meso or anthracene), 8.56 (s, 1H, meso or anthracene), 8.41 (d, 1H, anthracene), 8.22 (d, 1H, anthracene), 7.84 (d, 1H, anthracene), 7.66 (t, 1H, anthracene), 7.15 (t, 1H, anthracene, buried under solvent peak), 6.76 (d, 1H, anthracene), 4.1–3.2 (m, 16H, $-CH_2CH_3$), 3.10 (s, 6H, $-CH_3$), 2.75 (s, 6H, $-CH_3$), 2.34 (s, 6H, $-CH_3$), 2.00 (s, 6H, $-CH_3$), 1.59 (t, 6H, $-CH_2CH_3$), 1.51 (t, 6H, $-CH_2CH_3$), 1.33 (t, 6H, $-CH_2CH_3$), 1.29 (t, 6H, $-CH_2CH_3$), -7.80 (t, 3H, $-CH_2CH_3$, axial ligand), -8.49 (q, 2H, $-CH_2CH_3$, axial ligand); UV/vis (C_6H_6) λ_{max} 344, 394 (Soret), 530, 560 nm; MS *m/e* 1406 (cluster, $M^+ - 1$).

Acknowledgment. The support of the National Science Foundation is gratefully acknowledged. We thank H. T. Fish for providing the ligands H_4DPA and $H_4DPA(TMP)$ that are used in these studies. We acknowledge the Mass Spectrometry Facility of the University of California at San Francisco, supported by NIH Division of Research Resources Grant RR01614 and by NSF Grant DIR8700766.

Supplementary Material Available: Rotating-ring-disk voltammograms of $Ir(OEP)CH_2Ph$ and $Ir(TPP)H$ (2 pages). Ordering information is given on any current masthead page.

IC941325H